A regulatory module controlling GA-mediated endosperm cell expansion is critical for seed germination in Arabidopsis

Sánchez-Montesino, Rocío; Bouza-Morcillo, Laura; Marquez, Julietta; Ghita, Melania; Duran-Nebreda, Salva; Gómez, Luis; Holdsworth, Michael J.; Bassel, George; Oñate-Sánchez, Luis

DOI:
10.1016/j.molp.2018.10.009

Document Version
Peer reviewed version

Citation for published version (Harvard):
Sánchez-Montesino, R, Bouza-Morcillo, L, Marquez, J, Ghita, M, Duran-Nebreda, S, Gómez, L, Holdsworth, MJ, Bassel, G & Oñate-Sánchez, L 2019, 'A regulatory module controlling GA-mediated endosperm cell expansion is critical for seed germination in *Arabidopsis*', *Molecular Plant*, vol. 12, no. 1, pp. 71-85. https://doi.org/10.1016/j.molp.2018.10.009

Accepted Manuscript

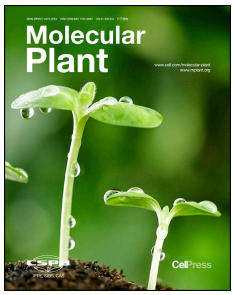

A regulatory module controlling GA-mediated endosperm cell expansion is critical for seed germination in Arabidopsis

Rocío Sánchez-Montesino, Laura Bouza-Morcillo, Julietta Marquez, Melania Ghita, Salva Duran-Nebreda, Luis Gómez, Michael J. Holdsworth, George Bassel, Luis Oñate-Sánchez

PII: S1674-2052(18)30335-6
DOI: https://doi.org/10.1016/j.molp.2018.10.009
Reference: MOLP 679

To appear in: *MOLECULAR PLANT*
Accepted Date: 31 October 2018

Please cite this article as: **Sánchez-Montesino R., Bouza-Morcillo L., Marquez J., Ghita M., Duran-Nebreda S., Gómez L., Holdsworth M.J., Bassel G., and Oñate-Sánchez L.** (2018). A regulatory module controlling GA-mediated endosperm cell expansion is critical for seed germination in Arabidopsis. Mol. Plant. doi: https://doi.org/10.1016/j.molp.2018.10.009.

A regulatory module controlling GA-mediated endosperm cell expansion is critical for seed germination in *Arabidopsis*.

Rocío Sánchez-Montesino[1], Laura Bouza-Morcillo[1], Julietta Marquez[2], Melania Ghita[2], Salva Duran-Nebreda[3], Luis Gómez[1,4], Michael J. Holdsworth[2]*, George Bassel[3]* and Luis Oñate-Sánchez[1]*.

[1]*Centro de Biotecnología y Genómica de Plantas, (Universidad Politécnica de Madrid –Instituto Nacional de Investigación y Tecnología Agraria y Alimentaria), Campus de Montegancedo, Pozuelo de Alarcón, 28223, Madrid, Spain.*

[2]*School of Biosciences, University of Nottingham, Loughborough LE12 5RD, UK.*

[3]*School of Biosciences, University of Birmingham, Birmingham B15 2TT, UK*

[4]*Departamento de Sistemas y Recursos Naturales, E.T.S.I. Montes, Forestal y del Medio Natural, Campus de Moncloa, 28040 Madrid, Spain*

**Authors for correspondence: Michael.Holdsworth@nottingham.ac.uk; g.w.bassel@bham.ac.uk; luis.onate@upm.es* (primary contact)

Running title: Endosperm cell expansion controls seed germination

Short Summary: This study demonstrates that endosperm cell expansion is crucial for germination and two NAC transcription factors play pivotal roles in this process. NAC25 and NAC1L act downstream of GAs and the RGL2 DELLA protein to upregulate cell-wall remodelling enzyme gene expression.

ABSTRACT

A key component of seed germination is the interplay of mechanical forces governing embryo growth and the surrounding restraining endosperm tissue. Endosperm cell separation is therefore thought to play a critical role in the control of this developmental transition. Here we demonstrate that in *Arabidopsis thaliana* seeds, endosperm cell expansion is a key component of germination. Endosperm cells expand to accommodate embryo growth prior to germination. We show that this is an actively regulated process supported by spatiotemporal control of the cell expansion gene *EXPANSIN 2* (*EXPA2*). The NAC transcription factors NAC25 and NAC1L were identified as upstream regulatory effectors of *EXPA2* expression, GA-mediated endosperm expansion and seed germination. The DELLA protein RGL2 repressed activation of *EXPA2* promoter by NAC. Our findings demonstrate a key role of this gene network in regulating endosperm cell-expansion to control the seed to seedling transition.

Keywords: cell expansion, cell wall remodelling enzymes, endosperm, expansin, NAC transcription factors, seed germination.

INTRODUCTION

In multicellular organisms, the regulation of growth requires a precise coordination between cell division and cell expansion. In the case of plants, the presence of a cell wall and absence of cell movement largely influence their ability to grow (Coen et al., 2004). Therefore, plants require mechanisms to modify the physical properties of their cell walls according to tissue-specific growth rates and developmental stages as well as in response to environmental cues.

Seed germination in *Arabidopsis thaliana* (hereafter Arabidopsis) is a useful system to study growth regulatory mechanisms since the developmental transition from seed to seedling is driven exclusively by cell shape change in the absence of cell division (Holdsworth et al., 2008; Sliwinska et al., 2009). The ability of seeds to germinate is thought to result from a balance between physical restrictions imposed by the embryo-surrounding tissues (testa and endosperm) and the ability of the embryo to grow and protrude (Finch-Savage and Leubner-Metzger, 2006; Holdsworth et al., 2008). The impact of endosperm on plant survival and seed vigour has been well documented (Bassel, 2016; Finch-Savage and Bassel, 2016), and it was shown that it has the capacity to communicate bidirectionally with the embryo (Groot and Karssen, 1987; Bassel et al., 2006; Lee et al., 2010), e.g., by influencing initial embryo growth (Lee et al., 2012b) or even by inhibiting germination altogether (Bethke et al., 2007; Lee et al., 2010). The decline in the mechanical resistance of the micropylar endosperm (the endosperm covering the radicle tip) leading to endosperm cell separation appears to be a general prerequisite for radicle (root tip) protrusion (germination *sensu stricto*) (Yan et al., 2014b; Steinbrecher and Leubner-Metzger, 2016).

In a number of plant species (including Arabidopsis) endosperm cell separation precedes germination, a process stimulated by gibberellins (GAs) that regulate the coordinated expression of cell wall remodelling enzymes (*CWREs*) which correlates with cell dissociation (Groot and Karssen, 1987; Chen and Bradford, 2000; Dubreucq et al., 2000; Chen et al., 2002; Müller et al., 2006; Penfield et al., 2006; Morris et al., 2011; Endo et al., 2012; Lee et al., 2012a; Martínez-Andújar et al., 2012; Yan et al., 2014a; Scheler et al., 2015;

Sechet et al., 2016). However, molecular mechanisms linking GA action with *CWRE* expression and the effect of CWREs on endosperm functionality and germination remain poorly understood.

In order to better understand the relationship between embryo growth and endosperm functionality, we investigated the biophysical and molecular events that take place within cells of the endosperm during Arabidopsis seed imbibition prior to radicle protrusion. This analysis identified the necessity of endosperm expansion for the completion of germination. Functional and genetic consequences underpinning these events were investigated, revealing a GA-mediated network of transcription factor (TF) regulated CWRE action.

RESULTS

Endosperm cells expand during germination. We examined endosperm cell expansion dynamics during seed germination using confocal microscopy and quantitative image analysis prior to radicle protrusion. Specifically, changes in endosperm cell geometry before (6 hours after imbibition; hai) and after (27 hai) testa rupture were analyzed. Confocal z-stacks of seeds with testa removed were taken to study the underlying endosperm (Figure 1A). Using 2.5 D image analysis, the size of endosperm cells was determined by cell segmentation (Figure 1B) and area analysis (Figure 1C) in MorphoGraphX (Barbier de Reuille et al., 2015). The endosperm was divided into 4 regions corresponding to the different anatomical parts of the underlying embryo it encapsulates (Figure 1D): radicle tip (micropylar endosperm, ME; region 1); radicle and lower hypocotyl (adjacent ME; region 2); hypocotyl (peripheral endosperm, PE; region 3); and cotyledons (cotyledon PE; region 4). Statistical analysis of the changes in cell surface area in these different regions before and after testa rupture identified significant differences in cell size for each region (Figure 1E). Endosperm cell growth was greatest in regions overlying the radicle and lower hypocotyl, which is consistent with these being previously identified as the sites of cell expansion in the underlying embryo (Bassel et al., 2014).

To visualize changes in endosperm cells during Arabidopsis seed germination, we prepared microscopic sections of seeds before and after testa

rupture. A concomitant formation of central vacuoles in the embryo and endosperm cells was seen at the time of testa rupture (Supplemental Figure 1A and 1B), reflecting reserve mobilization and resulting in vacuolation of protein storage vacuoles (Penfield et al., 2004; Bethke et al., 2007). When using a transgenic line with GFP targeted to the tonoplast (Cutler et al., 2000) early stages of germination showed a high density of vacuoles representing the multiple protein storage vacuoles present at this stage (Supplemental Figure 1C). Progressive formation of a large central vacuole was observed during the later stages of germination, co-incident with endosperm cell expansion (Supplemental Figure 1D). These results suggest that the observed subcellular events in the endosperm reflect those occurring in the embryo (Sliwinska et al., 2009) and are linked to endosperm cell expansion.

***EXPA2* is an endosperm-specific *CWRE* marker of cell expansion.** Previous work has shown that the expression of many CWREs, promoted by GAs, correlates with endosperm cell separation (Morris et al., 2011; Endo et al., 2012; Dekkers et al., 2013; Steinbrecher and Leubner-Metzger, 2016). Wherever cells are growing or modifying their cell walls, one or more expansin genes are usually involved (Cosgrove, 2015). *EXPANSIN 2* (*EXPA2*, At5g05290) encodes an endosperm-specific alpha-expansin induced by GAs, not repressed by ABA, under the control of DELLAs and with a proven genetic role in enhancing germination (Ogawa et al., 2003; Cao et al., 2006; Penfield et al., 2006; Morris et al., 2011; Endo et al., 2012). For these reasons, we decided to study the temporal and spatial expression kinetics of *EXPA2* in the context of endosperm expansion prior to germination.

We generated transgenic seeds containing a 2 kb *EXPA2* promoter (upstream of the ATG) fused to the β-glucuronidase gene (GUS) in a Col-0 background (*ProEXPA2:GUS*). Seeds were imbibed and endosperms separated from embryos at different times (6, 12, 18 and 24 hai) and assayed for histochemical staining to assess the temporal and spatial expression pattern in the endosperm (no GUS staining was observed in the embryo as this gene is endosperm-specific; Supplemental Figure 2). Initially, we analysed expression driven by this promoter in the endosperm of intact seeds. As shown in Figure 2A, GUS expression was observed by 18 hai in the endosperm region overlying

the radicle and lower hypocotyl, and subsequently extended along the region overlying the hypocotyl. This spatiotemporal activity of the *EXPA2* promoter overlaps the dynamics of endosperm expansion prior to germination (Figure 1E). Histochemical staining of the *ProEXPA2:GUS* seeds in the presence or absence of ABA, PAC and PAC+GAs, confirmed that *EXPA2* promoter activity in the endosperm depends on GAs and cannot be repressed by ABA (Figure 2B).

The endosperm perceives environmental signals that affect germination control (Lee et al., 2010). Communication with the embryo is bidirectional and endosperm cell separation requires a signal from the embryo (Groot and Karssen, 1987; Morris et al., 2011; Bassel, 2016). To determine whether *EXPA2* promoter activity depends on an embryo signal and its timing, endosperms were separated from embryos at different times during early seed imbibition (45, 60, 75 and 90 min after imbibition) and subsequently incubated isolated from the embryo for a total of 24 h to allow completion of downstream gene expression programmes. This analysis shows that GUS expression, driven by the *EXPA2* promoter relies on an inductive signal that is initiated between 45-60 min after imbibition of the seed (Figure 2C).

The *EXPA2* promoter contains a conserved sequence required for binding and transactivation by two NAC transcription factors. The above results prompted us to identify *cis*-elements controlling *EXPA2* promoter and upstream transcriptional regulators. We used a phylogenetic shadowing approach (Castrillo et al., 2011) with orthologous *EXPA2* gene promoters to define conserved *cis*-elements. An 80 bp sequence was identified (*EXPA2*-CS) with almost 50% overall identity among the eight species analysed (Supplemental Figure 3). Transgenic seeds carrying a luciferase reporter gene under the control of the *EXPA2-CS*, or a minimal promoter (control), were used to quantify luciferase expression *in vivo* (Figure 3A). The *4xEXPA2-CS* construct was able to increase luciferase expression 6-fold over the control construct 24 hai, suggesting that the *EXPA2-CS* is bound by TFs that activate gene expression in seeds (Figure 3B).

To identify TFs able to regulate *EXPA2* expression through binding to the *EXPA2-CS*, we used the *EXPA2-CS* sequence as bait to screen a library of

Arabidopsis TFs in a yeast one hybrid system (Castrillo et al., 2011; Sánchez-Montesino and Oñate-Sánchez, 2017; Sánchez-Montesino and Oñate-Sánchez, 2018). Only two yeast strains contained inserts able to activate the reporter gene (*HIS3*) under the control of the *EXPA2-CS* and to grow on the screening medium (Supplemental Figure 4A). Isolation and sequencing of the corresponding GAL4AD-TF plasmids showed that they contained two NAC TFs, hereafter NAC25 (*At1g61110*) and NAC1-like (NAC1L; *At3g12977*).

Two putative NAC-binding sequences (NACbs; 5´-ACGGAATT-3´) were identified in the *EXPA2-CS* and a mutated version containing 2 bp changes in the core sequence (Puranik et al., 2012; Franco-Zorrilla et al., 2014) of each NACbs was generated (*EXPA2-CSm*; Figure 3C). Diploid cells containing the *EXPA2-CS* bait and AD-NAC25 or AD-NAC1L were able to grow in the presence of 3-AT (a competitive inhibitor of the product of the *HIS3* gene) at concentrations blocking the growth of cells harbouring control plasmids (AD-∅ and AD-GFP; Figure 3D). No differences in growth with control yeast cells were observed when the *EXPA2-CSm* or a GA-responsive sequence present in the promoters of genes expressed in the epidermis of the embryo (*LIP1-CS*; Rombolá-Caldentey et al., 2014) were used as bait (Figure 3D and Supplemental Figure 4B). In conclusion, our results indicate that both NAC TFs bind the *EXPA2-CS* in yeast and that integrity of the core NACbs is required for their binding.

To determine the relevance of the NACbs for NAC transactivation of the *EXPA2* promoter, we carried out transient expression analyses *in planta.* As reporters, we fused the same initial 2 kb *EXPA2* promoter (see Figure 2) to the luciferase reporter gene (*ProEXPA2*). We also generated a 2 kb *EXPA2* promoter version containing the same NACbs mutations shown in Figure 3C (*ProEXPA2m*). As effectors, we cloned the two NAC ORFs under the control of the *35S* promoter (Figure 3E). *Nicotiana benthamiana* leaves were then infiltrated with different combinations of *Agrobacterium tumefaciens* cultures carrying reporters and effectors. Both NAC TFs were able to increase *ProEXPA2* expression but not that of the mutated version (*ProEXPA2m*), indicating that intact NACbs are required for full transactivation mediated by the NAC TFs *in planta* (Figure 3F).

The NACbs mediate GA responses and the RGL2 DELLA protein represses NAC-mediated transactivation. Endosperm cell separation and *EXPA2* upregulation are both GA-mediated processes (Ogawa et al., 2003; Penfield et al., 2006; Holdsworth et al., 2008; Yan et al., 2014a; Yan et al., 2014b). To analyze the role of the NACbs in the GA-mediated induction we generated transgenic seeds containing either *EXPA2-CS* or *EXPA2-CSm* fused to luciferase (*LUC*). High levels of luciferase activity were detected at 24 hai in control conditions but were reduced by almost 8-fold in the presence of paclobutrazol (PAC), an inhibitor of GA biosynthesis (Figure 4A). In addition, luciferase levels in seeds imbibed with PAC but supplemented with GA were similar to those in the control. Seeds carrying the *EXPA2-CSm* showed much lower basal expression and did not exhibit responsiveness to GA. These results indicate that transcription driven by the *EXPA2-CS* is modulated in response to GA and mediated by the NACbs.

To determine if the NACbs plays a broader role in GA-regulated gene expression, we looked for enrichment of the NACbs (5´-ACGGAATT-3´) in the promoters of genes represented in transcriptomes of germinating wild-type seeds compared with the GA-deficient *ga1-3* mutant (Koornneef and van der Veen, 1980; Sun and Kamiya, 1994) and the *ga1-3 gai-t6 rga-t2 rgl1-1 rgl2-1* mutant lacking four DELLA genes (Cao et al., 2006). The average occurrence of the NACbs sequence was found to be significantly higher in GA-upregulated (GAup) and DELLA-downregulated (DELLAdown) gene promoters when compared with the control (Figure 4B). When the occurrence of a monocot GA-responsive *cis*-element (GARE) (Skriver et al., 1991; Gubler and Jacobsen, 1992) was analyzed in these gene promoters, no significant enrichment was found (Ogawa et al., 2003; Rombolá-Caldentey et al., 2014).

We analysed the molecular mechanism mediating GA responsiveness of the *EXPA2* promoter. Our results clearly indicate a role of the NACbs sequence in GA responses (Figure 4A and 4B). One possibility could be that DELLA proteins block NACbs-mediated gene expression by sequestering NACs in a physical interaction. To test this possibility, the coding sequence for the RGL2 protein, the predominant DELLA repressor of seed germination in Arabidopsis (Lee et al., 2002; Tyler et al., 2004; Cao et al., 2005), was fused to the GAL4 DNA binding domain and used as bait for yeast two hybrid experiments. Yeast

cells carrying BD-RGL2 and the AD-NAC25 construct, but not those harbouring the control plasmids or the AD-NAC1L construct, were able to grow on the selection medium in the presence of 3-AT (Figure 4C), indicating that NAC25 is able to interact with the RGL2 protein. To validate this protein interaction *in planta*, we carried out co-immunoprecipitation experiments using HA and GFP translational fusions of *NAC25* and *RGL2*, respectively. As shown in Figure 4D, the HA-NAC25 protein was detected by the anti-HA^{HRP} antibody only in protein extracts that had been agroinfiltrated with the corresponding construct (α-HA panels, lanes 2,3,5 and 6) and the HA epitope fused to the NAC25 protein was efficiently immunoprecipitated by the anti-HA antibody (α-HA panels, lanes 5 and 6). Likewise, the anti-GFP^{HRP} antibody successfully detected the RGL2-GFP hybrid protein (α-GFP panel, lanes 1 and 3). Since the RGL2-GFP protein was detected after the HA-NAC25 was immunoprecipitated with the anti-HA antibody (α-GFP panel, lane 6), these results demonstrate that NAC25 interacts with RGL2 *in planta*.

To measure the effect of this interaction on the transactivation ability of NAC25 we carried out transient expression assays. As shown in Figures 4E and 4F, RGL2 is unable to regulate *EXPA2* expression on its own, but efficiently blocks NAC25 mediated transactivation. It has been demonstrated that *EXPA2* and *RGL2* are expressed in the seed endosperm (Penfield et al., 2006; Lee et al., 2010; Yan et al., 2014a; this paper). To check for expression of *NAC* genes in the endosperm, we isolated RNA from Arabidopsis embryos and endosperms dissected at different times upon seed imbibition and quantified their mRNA expression by RT-qPCR. Our results (Supplemental Figure 5) show that *NAC25* and *NAC1L* are expressed in both tissues at early timepoints but mainly in endosperm at later timepoints, indicating that this regulation is meaningful in the context of seed germination.

NAC25 and NAC1L are positive regulators of seed germination and *CWRE* gene expression. To analyse the role of these TFs *in planta*, we characterised the seed germination properties of two single loss-of-function mutants for the *NAC25* and *NAC1L* genes (Supplemental Figure 6 and Supplemental Table 1). Mutation of either gene led to delayed germination when compared to the wild-type (Figure 5A), indicating that both NAC TFs are positive regulators of this

process. To identify other genes regulated by the NAC TFs we compared gene expression during seed germination in the *nac25* and *nac1L* null mutants and wild-type controls using deep sequencing of RNA populations (RNA-seq). Analyses of RNA-seq results led to the identification of NAC25 and NAC1L-regulated genes (Supplemental Table 2). When genes differentially regulated over 2-fold were considered, we identified 1,260 and 2,094 genes as putative NAC1L and NAC25 regulated genes, respectively (Figure 5B). In both null mutants most genes were downregulated accounting for up to 88% in *nac1L-1* (1,109 DOWN and 151 UP) and 94.5% in *nac25-1* (1,980 DOWN and 114 UP) suggesting that both genes are positive regulators of gene expression. The ratio of downregulated to upregulated genes in both transcriptomes increased when only genes differentially regulated above 4-fold were considered, further highlighting the role of both NAC proteins as activators of gene expression. Importantly, the overwhelming majority of *nac1L-1* downregulated genes (93%) were commonly downregulated in *nac25-1*, while almost 48% of *nac25-1* downregulated genes were specific for this mutant. These data suggest that *NAC25* has a wider regulatory role than *NAC1L* and that *NAC1L* lies in the same regulatory pathway. In agreement with these results, a *nac25-1 nac1L-1* double mutant produced a similar germination delay to those observed for the single mutants (Figure 5C). Thus, NAC25 and NAC1L could share regulatory roles by forming a protein complex through physical interaction. Our results using the Y2H system indicate that NAC25 and NAC1L are able to form homo and heterodimers (Figure 5D). To validate these protein interactions *in planta*, bimolecular fluorescence complementation (BiFC) experiments were performed by agroinfiltration of *N. benthamiana* leaves. The NAC CDSs were translationally fused to the N-terminal half of the yellow fluorescent protein (N-YFP) or the C-terminal half of the cyan fluorescent protein (C-CFP) as indicated in Supplemental Figure 7. A strong fluorescent signal was observed in nuclei of *N. benthamiana* cells for every co-infiltration containing pairs of NAC translational fusions but not with controls. These results indicate that NAC25 and NAC1L can interact *in planta* and support our genetic evidence indicating they could be essential components of the same regulatory complex.

We carried out gene ontology analyses using genes downregulated at least 4-fold in *nac25-1*. We could observe overrepresentation of genes related

to growth and cell wall modification and response to GAs (Supplemental Table 3), two biological processes playing a central role in germination and endosperm function. RT-qPCR analyses for some of those genes confirmed their downregulation (Supplemental Figure 8). These analyses showed that *EXPA2* is strongly downregulated in both *nac25-1* (almost 30-fold) and *nac1L-1* (almost 20-fold) mutants, confirming our discovery of *EXPA2* promoter activation by these TFs. We compared the *nac25-1* downregulated transcriptome with transcriptomes related to GA responses during seed germination. Figure 5C shows that over 50% of the genes upregulated ≥4-fold by GAs (Cao et al., 2006) were also downregulated ≥4-fold in *nac25-1*. This percentage increased to almost 70% when genes with 2-fold changes were compared (Supplemental Figure 9). In contrast, almost no overlap was observed with genes repressed by GAs. According to the results of Cao et al. (2006), almost 90% of the GA induced genes (≥4-fold) were downregulated by DELLAs (DELLAdown) and we observed that over 50% of the DELLAdown genes were also downregulated in *nac25-1*. Stamm et al. (2012) published a list of genes specifically downregulated by RGL2, the major DELLA repressor of seed germination, and over 30% of them (≥4-fold) were also downregulated in *nac25-1*. No overlap was observed when GA-related transcriptomes from buds were compared (Cao et al., 2006), suggesting that NAC25 regulation is seed-specific.

Eighty five genes related to cell wall modification were repressed > 2-fold, including expansins, xyloglucan endotransglucosylases, pectin methylesterases and arabinogalactans, and most were inducible by GA under the control of DELLA (Supplemental Table 4) according to published transcriptomes (Ogawa et al., 2003; Cao et al., 2006; Stamm et al., 2012; De Giorgi et al., 2015). When the 500 bp promoters of the 85 *CWRE* genes (Supplemental Table 4) were analyzed, a significant enrichment of the NACbs was observed (Figure 5D). This enrichment was higher than that found in other transcriptomes, suggesting that many *CWRE* genes could be direct targets of NACs. However, no NACbs enrichment was observed in the *nac25-1* downregulated genes, compared to TAIR, suggesting that other proteins might be involved in their regulation (Supplemental Table 5).

***NAC25* and *NAC1L* positively regulate endosperm cell expansion.** To assess the effect of NAC25 and NAC1L on endosperm physical properties, we measured endosperm cell expansion in imbibed WT, *nac25-1* and *nac1L-1* seeds. Since testa rupture is an early marker of germination, we determined the rupture kinetics in the genotypes under study. By 27 and 32 hai, testa rupture had occurred in 20 to 50% of WT, while it was almost negligible for the mutant seeds (Figure 6A). Next, we removed the testa of seeds at 6 and 27 hai and subjected them to confocal laser scanning microscopy and 3D reconstruction, segmentation and clustering. Quantification of changes in cell surface area in the four endosperm regions was performed (Figure 6B). Wild-type seeds increased endosperm cell surface in all regions examined, the highest increase being observed in regions 1 and 2 (70%) followed by regions 4 (44%) and 3 (26%). *nac25-1* and *nac1L-1* seeds however did not show any significant increase in cell surface in any of the areas examined at the studied time points. These quantitative analyses of cell shape changes indicate that these NAC TFs regulate endosperm cell expansion.

DISCUSSION

This study provides new insights into the biophysical and molecular network underlying endosperm function in regulating Arabidopsis seed germination. While it has been clearly established that endosperm cell separation is important in the control of germination, our observation of endosperm expansion during imbibition represents a previously undescribed necessary regulatory step in this developmental transition. This provides an important advance in our understanding of germination biology. In addition, we identified a gene network including previously undescribed genetic factors controlling endosperm expansion by modulation of CWREs function.

By measuring changes in endosperm cell surface area using confocal imaging and 3D geometry reconstruction, we observed that all endosperm cells expand during imbibition but at different rates. The rate of expansion is greatest in the regions covering the radicle and lower hypocotyl, which coincides with the

site of testa rupture and the highest expansion rates of the embryo axis (Stamm et al., 2017). These results highlight the different roles of the distinct regions of the endosperm.

Two NAC domain TFs (NAC25 and NAC1L) were identified as upstream regulatory factors controlling the expression of the *EXPA2* gene and regulating endosperm expansion prior to germination. Both transcription factors bind to a conserved *cis*-element within the *EXPA2* promoter and activate transcription. The observed strong downregulation of *EXPA2* in *nac25/1L* mutant transcriptomes also confirms the importance of these transcription factors in regulating *EXPA2* RNA accumulation *in vivo*. Neither *NAC25* nor *NAC1L* are endosperm-specific at the RNA level, suggesting that other factors are also important in contributing to the endosperm-specificity of *EXPA2* expression, perhaps through interaction with other *cis*-elements in the *EXPA2* promoter. Despite NACs are mainly expressed in endosperm after 6 hai, some of the *CWRE* downregulated genes shown in Table S4 have been described as embryo-specific (Dekkers et al., 2013), and therefore, we cannot rule out the possibility that some of the phenotypes observed in the nac mutants could be partly due to reduced embryo growth. GA is a key positive regulator of endosperm function in the germination process, and DELLA regulators repress GA responses. We found that the major germination-associated DELLA, RGL2, interacts with NAC25 *in vivo*, and also inhibits the NAC25-activation of the *EXPA2* promoter. This provides a simple mechanism for the regulation of EXPA2 transcription (Figure 7) where in low GA situations (e.g. dormant seeds) RGL2 would sequester NAC25, thereby inhibiting *EXPA2* transcription. In high GA situations (eg leading to germination) GA-mediated destruction of RGL2 would allow NAC25 to interact with the *EXPA2* promoter and thereby enhance *EXPA2* expression. We found that the NAC25 binding element NACbs was significantly enriched in *CWRE* promoters. This gene expression module (RGL2-NAC25-NACbs) could therefore effectively modulate the expression of a cohort of CWREs allowing expansion of the endosperm only in high GA situations, thus favoring subsequent germination. The endosperm cell expansion observed in WT seeds is blocked when NAC25 and NAC1L activity is removed, demonstrating their importance in controlling this process. De Giorgi et al. (2015) reported endosperm cell expansion in the micropylar and

peripheral endosperm using seed histological sections and identified a role for cutin biosynthetic genes (*BDG1*, *LACS2*) in preventing cell expansion in imbibed seeds under low GA conditions. However, we observed that in *nac* mutants *BDG1* and *LACS2* were downregulated (Supplemental Table 2) and *nac* mutant transcriptomes and phenotypes resembled phenotypes of reduced GA-signalling. This suggests that the increased cell expansion observed in *bdg1* and *lacs2* depends on additional NAC-upregulated genes.

Germination involves bidirectional interactions between the embryo and endosperm (Yan et al., 2014b). Endosperm cell separation requires the presence of the embryo, pointing to the existence of a diffusible signal from the embryo (Groot and Karssen, 1987; Groot et al., 1988; Müller et al., 2006). We showed that a signal requiring the embryo is perceived by the endosperm between 45-60 minutes after the initiation of seed imbibition, that activates the *EXPA2* promoter. The strength of GUS staining comparing endosperms from intact and separated seeds suggests that continued signaling is required for maximal *EXPA2* promoter-driven expression. The nature of the initial signal is unknown and could be chemical, mechanical or a combination of both. Genetic programs underpinning endosperm expansion, in addition to endosperm cell wall separation, also therefore depend upon mobile signal(s) requiring the embryo.

Previously, we described a molecular mechanism responsible for GA-signalling in the embryo that involved two HD-ZIP TFs expressed in the epidermis (Rombolá-Caldentey et al., 2014). We have found that when GA-signalling is blocked in the embryo epidermis during seed imbibition, *EXPA2* expression is not affected (Supplemental Figure 10), suggesting that GA-signalling in endosperm does not require a fully functional GA-signalling in embryo epidermis. These results are in line with previous findings pointing to different molecular mechanisms driving GA responses depending on the cell layer and developmental phase (Penfield et al., 2006; Ubeda-Tomas et al., 2008; Lee et al., 2010; Heo et al., 2011; Zhang et al., 2011; Duan et al., 2013; Geng et al., 2013; Lofke et al., 2013; Rombolá-Caldentey et al., 2014).

This study identifies endosperm expansion during imbibition as a necessary key step in the regulation of germination and defines its control by an

embryo initiated gene network. This provides an important insight into the regulatory processes that underpin the seed to seedling transition in plants.

METHODS

Plant materials. Plants were germinated either on Petri dishes containing half-strength Murashige and Skoog (MS) medium buffered with 2 mM MES, pH 5.7, and 0.7% (w/v) agar or in soil and grown to maturity at 16 h of light at 22℃/8 h of dark at 20℃ and 60% relative humidity. Seeds we re harvested when plants had ceased flowering and siliques were starting to dehisce. Wild type and mutant plants were in the Col-0 ecotype. NAC25 loss-of-function mutants were SM_3_16875 (KO1) and SM_3_37315 (KO2). NAC1L loss-of-function mutants were SALK_063384 (KO1) and SALK_049270 (KO2). Genotyping of the mutants was carried out by PCR amplification of gDNA using appropriate primer combinations (Supplemental Table 1). gDNA was isolated as described by Edwards et al. (1991). Appropriate constructs were introduced into *A. thaliana* (Col-0 ecotype) using the *Agrobacterium tumefaciens* strain GV3101 and the floral-dip method (Clough and Bent, 1998).

Sources of orthologous *EXPA2* gene promoter sequences from several *Brassicaceae* species, phylogenetic and bioinformatic analyses. Oligonucleotides to amplify *EXPA2* orthologous promoter sequences from *Descuriainia sophia*, *Carrichtera annua*, *Hornungia petraene* and *Brassica oleracea* were designed as described in Castrillo et al. (2011) and are listed in Supplemental Table 1 (EXPA2-rev and At5g05280-fw). The promoter sequence corresponding to the *A. thaliana EXPA2* gene was downloaded from the TAIR webpage using the bulk data retrieval tool (https://www.arabidopsis.org/tools/bulk/sequences/index.jsp). Orthologous promoter sequences from *Arabidopsis lyrata*, *Thelungiella halophila* and *Capsella rubella* were downloaded from the Phytozome webpage (https://phytozome.jgi.doe.gov/pz/portal.html). Alignment of promoter sequences and detection of conserved blocks were carried out as described in

Castrillo et al. (2011). NACbs occurrence in promoters of genes differentially expressed in GA-related transcriptomes was calculated as described previously (Rombolá-Caldentey et al., 2014).

In Vivo Imaging of Bioluminescence. *In vivo* imaging and quantification of luciferase activity were carried out using a cooled CCD camera (NightOwl II LB 983 NC-100; Berthold Technologies) and the provided software. Seeds from representative lines were simultaneously grown and sown on 0.6% agarose or MS agar plates in the presence or absence of 5 µM PAC or 5 µM PAC plus 5 µM GA. Plates were directly transferred to a chamber at a constant temperature of 22℃ and a photoperiod of 16 h of light/8 h of d ark for 24 or 48 h. Plates were then sprayed with 100 µM luciferin and imaged after 40 min.

Generation of constructs for yeast and plant assays. A 2,106 bp promoter fragment from the *AtEXP2* gene (containing the first three *EXPA2* ORF codons) was amplified by PCR from *A. thaliana* (Columbia ecotype) genomic DNA using the LO1884 and LO1885 primers (Supplemental Table 1) and recombined with the BP clonase enzyme mix into the pDONR221 plasmid (Invitrogen). This construct was recombined with the LR clonase enzyme mix into the pBGWL7 plasmid (VIB) containing the luciferase CDS to obtain the *ProEXPA2:LUC* construct or into the pKGWFS7 plasmid (Karimi et al., 2002) to obtain the *ProEXPA2:GUS* construct. To generate the mutated version of the *EXPA2* promoter (*ProEXPA2-mut:LUC*), two different primer pairs (LO1+LO1916 and LO1915+LO604) were used to amplify two partially overlapping fragments containing the mutated nucleotides and using the wild-type version cloned in pBGWL7 as a template. Fragments were digested with *AvrII* and ligated after purification. The resulting fragment was used as a template to amplify the mutated 2,106 bp fragment by using the primers LO1 and LO604. The PCR product was recombined with the BP clonase enzyme mix into the pDONR221 plasmid and then recombined with the LR clonase enzyme mix into the pBGWL7 plasmid.

To introduce four tandemly repeated *EXPA2-CS* into plants, we used a binary plasmid (pYRO) containing a luciferase (LUC+) CDS downstream of a minimal promoter sequence with *BamHI* and *HindIII* restriction sites at its 5´-end

(*min:LUC or* -58F8-pYRO; Chen and Singh, 1999; Castrillo et al., 2011). The *ProEXPA2* construct in the pDONR221 plasmid was used as template to amplify the *EXPA2-CS* using the primers LO839 and LO840 that contained *Bgl2* and *BamH1*/Hind3 restriction sites, respectively (Supplemental Table 1). Then, the engineered *Bgl2* and *Hind3* sites of the *EXPA2-CS* were used to clone it into the *BamH1* and *Hind3* sites of the *min:LUC* plasmid upstream of the minimal promoter and the LUC+ gene (*1xEXPA2-CS:LUC*). This process was repeated three more times to generate a *4xEXPA2-CS:LUC* plasmid. To produce the *4xEXPA2-CSm:LUC* construct, the *4xEXPA2-CSm* sequence (342 bp) was synthesized and cloned in the *BamHI*/*HindIII* sites of the pUC57 plasmid (GeneScript, USA). The *4xEXPA2-CSm* sequence was fused to the luciferase reporter gene by cloning into the *BamHI*/*HindIII* sites of the pYRO plasmid (*4xEXPA2-CSm:LUC*).

For yeast assays, the *ProEXPA2* fragment in the pDONR221 plasmid was used as template for PCR amplification of the *EXPA2-CS* with the LO1201 and LO1202 primers (Supplemental Table 1). The amplified fragment was cloned into the *Xba1* and *Xma1* sites of the pTUY1H plasmid (Castrillo et al., 2011). To generate the *EXPA2-CSm* version, three different primer pairs (LO1040+LO1914, LO1913+LO1912 and LO1911+1041) were used to amplify three partially overlapping fragments containing the mutated nucleotides in the NACbs core sequence (5´-CGT[G/A]-3´; (Puranik et al., 2012; Franco-Zorrilla et al., 2014) and using the wild-type version cloned in pTUY1H as a template. The generated fragments were purified and combined to serve as templates for the amplification of a 180 bp DNA sequence by using the primers LO1040 and LO1041. The 80 bp *EXPA2-CSm* was excised from the 180 bp fragment and cloned into the pTUY1H plasmid by using the *Xba1* and *Xma1* restriction enzymes. Full sequencing of the TFs isolated in the screening revealed that the first 9 bp of NAC25 open reading frame (coding for the first 3 aminoacids of the protein) were missing. The full version of NAC25 was PCR-amplified using a SSP pUNI clone (U605068; Yamada et al., 2003) as a template and primers LO1344 and LO1345. The resulting 972 bp ORF was cloned into pDONR221 by a BP recombination reaction and translationally fused to the GAL4AD by a LR reaction between the pDONR221-NAC25 and the pDEST22 or the pGADT7(GW) plasmids, or to the GAL4BD by using the pGBKT7(GW) as the

destination vector. The NAC1L ORF contained in the library prey plasmid (pDEST22; GAL4AD-NAC1L) was cloned into pDONR221 by a BP recombination reaction and transferred to the pGBKT7(GW) or pGADT7(GW) plasmids by a LR reaction. All control constructs and construct carrying GAL4BD-RGL2 (BD-RGL2) have been previously described (Rombolá-Caldentey et al., 2014).

For co-immunoprecipitation assays, the NAC25-pDONR221 vector (entry vector) was digested with the *MluI* enzyme at 37ºC for 2 hours before the LR recombination reaction with the pEarleyGate201 to obtain an N-terminal fusion to the HA epitope. The RGL2 ORF was obtained from the construct pDEST22-RGL2 isolated from the corresponding yeast strain in the in RR library (Castrillo et al., 2011) and transferred to pDONR207 by BP reaction. The RGL2 ORF was then transferred to the pMDC83 plasmid by a LR reaction to obtain a translational fusion to the complete sequence of the Green Fluorescent Protein (GFP).

For transient expression analyses, overexpression constructs for NAC25, NAC1L and RGL2 were generated by transferring their ORFs to the PCX plasmid from ORF-pDONR221 by LR reaction.

Transient expression analyses in *Nicotiana benthamiana*. The reporter constructs *ProEXPA2:LUC* and *ProEXPA2m:LUC* and the effector constructs (pCX plasmid) overexpressing NAC25, NAC1L and RGL2 were introduced into *Agrobacterium tumefaciens* C58 GV3101:pMP90 and the resulting strains were used for agro-infiltration of 4 weeks old *N. benthamiana* leaves. The empty pCX plasmid was used as negative control and a pBIN61-35S:P19 plasmid was always co-infiltrated to avoid gene silencing (Voinnet et al., 2003). All Agrobacterium cultures were used at OD_{600} = 0.3. Three days after inoculation luciferase activity was measured in 0.6% agarose microtiter plates as described in Espinosa-Ruiz et al. (2017), using a cooled CCD camera (NightOwl II LB 983 NC-100).

Co-immunoprecipitation assay (CoIP). For the co-immunoprecipitation assay, about 5 g of *N. benthamiana* leaves were ground in liquid nitrogen and homogenized in 5 ml of extraction buffer. Samples were centrifuged at 13,000

rpm at 4ºC for 10 minutes, the supernatants were filtered using miracloth paper (Calbiochem – 475855-1R) and transferred into a new tube. Also, as positive control, 75 µl of each protein extract were reserved, mixed with 25 µl of loading buffer 4x and 15 µl were loaded in the gel. Total protein concentration was determined by using the Bio-Rad Bradford Protein Assay Kit and 1 mg of total soluble proteins was used for further immunoprecipitation. Each protein extract was then incubated with 1 µl of Anti-HA antibody (1.9 µg/ µl; kindly provided by Dr. Salomé Prat; CNB) for 2 hours in a cold room. For protein immunoprecipitation, 20 µl of Dynabeads protein G (Life technologies) were cleaned with 50 µl of extraction buffer and then were added into the protein solution which had been previously incubated with the antibody. After 30 minutes of incubation at 4ºC, beads were separated from the protein extract with a magnet and washed four times with 500 µl of extraction buffer. Finally beads were collected and resuspended in 45 µl of extraction buffer, mixed with 15 µl of loading buffer, boiled at 95º C during 5 minutes and loaded in two gels. Interactions between fusion proteins HA:NAC25 and RGL2:GFP were detected by immunoblot with 1:1000 diluted anti-GFP^{HRP} (Miltenyi Biotec) and anti-HA^{HRP} (Roche) antibodies.

Bimolecular fluorescence complementation (BiFC) experiments. The NAC CDSs were translationally fused to the N-terminal half of the yellow fluorescent protein (N-YFP) or the C-terminal half of the cyan fluorescent protein (C-CFP) by using the Gateway binary destination vectors pNXGW or pCXGW, respectively. All Agrobacterium cultures were used at OD_{600} = 0.3 and agroinfiltration of *N. benthamiana* leaves was carried out as previously described (Rombolá-Caldentey et al., 2014). BiFC images were taken three days after agroinfiltration by using a Leica DM 2000 fluorescence microscope.

Germination and testa rupture assays. Testa and endosperm rupture (germination) were scored at the indicated timepoints in germination assays carried out as described in Rombolá-Caldentey et al. (2014).

Yeast transformation and one hybrid screening. For a complete description of the methodology and yeast strains used see Castrillo et al. (2011) and Sánchez-Montesino and Oñate-Sánchez (2017, 2018).

RNA isolation and RT-qPCR. RNA extraction was carried out as described previously (protocol 2 in Oñate-Sánchez and Vicente-Carbajosa, 2008) except that: in step 2, the mix containing the sample, phenol and chloroform was applied to a Phase Lock (5-PRIME) eppendorf previous to centrifugation to prevent organic contamination of the aqueous phase; in step 4, the RNA pellet was dissolved in 88 μl of water and 20 units of RNAse-free DNAse were used. First-strand cDNA synthesis and quantitative real-time PCR has been previously described (Rombolá-Caldentey et al., 2014). For RNA-sequencing, RNA isolation was followed by RNA cleanup by the RNeasy mini kit (Qiagen). Library construction and sequencing (mRNA-seq) on Illumina HiSeq2500 was carried out at CNAG (National Centre for Genomic Sequencing, Barcelona, Spain), resulting in 45-72 million 50 bp single reads per sample.

Sequence processing. We analyzed the global change of gene expression in WT (Col-0) and one representative KO for each *NAC* gene by carrying out RNA-seq of seeds at 12 hai. Total RNA from three biological replicates for each genotype was isolated and used to prepare their corresponding libraries for mRNA sequencing (Illumina HiSeq 2500 with v4 chemistry). A minimum of $45x10^6$ 50 bp single reads were obtained for each sample (Supplemental Table 6), aligning more than the 99.3% of reads per sample against the Araport11 reference genome. Transcript data were downloaded in FastQ format from the sequencing facility and the quality was assessed using FastQC v0.11.5 (http://www.bioinformatics.bbsrc.ac.uk/projects/fastqc). In order to evaluate the expression levels of the reads aligned, the cuffdiff protocol under local Galaxy interface v.2.2.1.0 (Afgan et al., 2016) was used. The reads were aligned against the genome using TopHat v2.1.0 (Langmead et al., 2009) and then the expression was obtained with Cuffdiff v2.2.1.3 (Trapnell et al., 2010). Classic-fpkm normalization method, per-condition estimation and bias correction were applied to the analysis. Only differentially expressed genes misregulated over 2-fold were considered for downstream analyses referring to genes as being KO-

up-regulated or KO-down-regulated only if the ratio of WT vs KOs was equal to or more than 2-fold different, with a p-value cut-off at 0.05. Using these criteria, we identified 1,260 and 2,094 genes as putative KO1 and KO2-regulated genes, respectively.

Measuring cell expansion by confocal imaging and geometry reconstruction. Seeds of each wild-type and mutant lines were sown on a filter paper placed onto 0.6% agarose plates, and transferred to a chamber at a constant temperature of 22℃ and a photoperiod of 16 h of light/8 h of dark. After 6 and 27 hai, testas from 5 seeds per line were carefully removed by using 2 forceps and immediately transferred to a fixative solution (ethanol:acetic acid 3:1). After incubation in fixative solution for at least 24 h, the fixative was replaced by clearing solution (0.2 M NaOH, 1% SDS) and incubated for one week. After repeating the clearing step, seeds were left in water for several days. Cell walls were stained using the mPA-PI procedure as described previously (Bassel et al., 2014). Before imaging, seeds were replaced in chloral hydrate clearing solution (4 g chloral hydrate : 1 ml glycerol : 2 ml water), and z-stacks were collected using a Zeiss LSM710 confocal microscope.

Image analysis was performed by using the MorphoGrapX software (Barbier de Reuille et al., 2015). After applying a Gaussian Blur Stack, a surface (mask) surrounding the seed was generated. The surface was first fitted and then signal emerging from the cell walls was projected in the surface. Then, surfaces were automatically segmented into cells and incorrectly segmented cells were manually discarded. Cell surfaces (μm^2) were obtained by a heat map tool. At least 180 cells from 5 different samples from every line and time after imbibition were used to determine differences in cell elongation. T-Student test was applied to the average data from 6 hai and 27 hai samples of every line, treated as independent lines. P-values lower than 0.05 were considered as indicative of a significant difference.

FUNDING

This work was supported with grants to L.O.-S by the Spanish Ministry of Economy and Competitiveness (BIO2013-46076-R and BIO2016-77840-R), by the Biotechnology and Biological Sciences Research Council [grant numbers

BB/J017604/1, BB/L010232/1, BB/N009754/1, BB/G02488X/1] to MJH and GWB, and Leverhulme Trust Grant RPG-2016-049 to GWB together with SDN.

AUTHOR CONTRIBUTIONS

R.S.-M performed most of the experiments, L.B.-M did the CoIP experiments and both were supervised by L.O.-S. Quantitative image analyses were carried out by R.S.-M and S.D.-N. under the supervision of G.B. GUS expression analyses were done by M.G and J.M under the supervision of M.H. L.G. helped with RNA-seq analyses and reviewing the manuscript. M.H., G.B. and L.O.-S. wrote the manuscript.

ACKNOWLEDGEMENTS

We wish to thank Dr. A. Muñoz for help with the alignment and evaluation of expression levels of the RNA-seq data, Dr. Javier Paz-Ares for providing some of the *EXPA2* promoter sequences used in phylogenomic analyses, Dr. Mónica Pernas for critical reading of the manuscript and Anne Medhurst for making the *ProEXPA2:GUS* construct. The NAC knock-out mutant seeds were obtained from NASC (http://arabidopsis.info). No conflict of interest declared.

FIGURE LEGENDS

Figure 1. Endosperm cell expansion is a key component of germination. **(A)** Confocal image of testa-removed seed. **(B)** Endosperm cell segmentation. **(C)** Segmented cells coloured by surface area (μm^2) as indicated by the scale bar. **(D)** Cells clustered in 4 regions. Region 1, marked in green colour, corresponds to the micropylar endosperm; region 2, coloured in blue, is the adjacent to the micropylar endosperm; region 3, tinted in yellow, refers to the peripheral endosperm; and region 4, in pink color, is the area surrounding the cotyledons. **(E)** Changes in endosperm cell surface (average percentage + SE) per region. Cell surfaces per region in samples at 27 hai were compared to those calculated in samples at 6 hai. Five Arabidopsis Col-0 seeds for each timepoint were analyzed. Asterisks represent significant differences at $P < 0.01$ (**) and at $P < 0.05$ (*) using the Mann-Whitney test (two-sided).

Figure 2. *EXPA2* spatio-temporal expression pattern is tightly associated with endosperm expansion and depends on embryo signal/s. (A) *ProEXPA2:GUS* seeds were imbibed on ½ MS medium for the indicated times and seed coats were removed and stained overnight to detect GUS activity. GUS staining was visualized after bleaching the testa. **(B)** *ProEXPA2:GUS* seeds were imbibed on ½ MS medium in the absence or presence of ABA (10µM), PAC (20µM) or PAC (20µM) plus GA (10µM) for 24 h. Seed coats were removed and stained overnight. **(C)** *ProEXPA2:GUS* seeds were imbibed on ½ MS medium and, at the indicated times (min, minutes), seed coats were separated from embryos, incubated on ½ MS for a total of 24 h and stained overnight.

Figure 3. Two NAC TFs bind to a conserved promoter sequence to activate *EXPA2* transcription. (A) Constructs used for functional analyses of the *EXPA2* conserved sequence (*EXPA2-CS*; black box); Minimal promoter (Min; grey box). **(B)** Seeds from two representative transgenic lines for each construct (Min or *4xEXPA2-CS)* were imbibed for 24 h. Average luciferase levels and SE for at least 10 seeds for each line are shown. **(C)** Sequence of the wild-type *EXPA2-CS* and a version mutated in the putative NAC binding sites (*EXPA2-CSm*). Mutated bases are indicated in lowercase. **(D)** Yeast strains containing one copy of the *EXPA2*-CS or *EXPA2-CSm* fused to the *HIS3* reporter gene were mated to strains containing the AD- ∅, AD-GFP, AD-NAC1L or AD-NAC25 constructs. Diploid cells were grown on diploid (-L-W) and screening (-L-W-H) plates with increasing concentrations of 3-AT. **(E)** Diagram of the *EXPA2* promoter (reporters) and TF constructs (effectors) used for transient expression analyses in *N. benthamiana* leaves. *N. benthamiana* leaves were agroinfiltrated with the *ProEXPA2* or the *ProEXPA2m* constructs together with each effector construct overexpressing the NAC25 or the NAC1L TFs. **(F)** Control is the empty effector plasmid (pCX) with each of the reporters. Averages and SE of luciferase activity from at least 6 replicates are shown and similar results were obtained in an additional agroinfiltration experiment. Asterisks represent significant differences at $P < 0.01$ (**) and at $P < 0.05$ (*) using the Mann-Whitney test (two-sided).

Figure 4. The NACbs mediates GA-responses and RGL2 represses NAC25 transactivation by physical interaction. (A) Seeds from transgenic lines with

a *4xEXPA2-CS* or a *4xEXPA2-CSm* promoter fused to luciferase were imbibed for 48 h in the absence (NT) or presence of PAC (5 µM) or PAC (50 µM) plus GA (5 µM). Luciferase levels and SE from at least 10 seeds for each line are shown. **(B)** NACbs sequence content in 500-bp promoters of genes upregulated (GAup) or downregulated (GAdown) in response to GA or in DELLA mutants (DELLAup or DELLAdown) as described by Cao et al. (2006). DELLAind, DELLA independent. The average NACbs occurrence in the Arabidopsis gene promoters, Araport11 Loci Upstream Seq–500 bp, is taken arbitrarily as 1. Asterisks represent significant differences, at $P < 0.01$ (**) or $P < 0.05$ (*), from the control (TAIR) using the X^2-test. **(C)** Yeast strains containing the RGL2 CDS fused to the GAL4-BD (BD-RGL2; bait) were mated to strains containing the AD-Ø, AD-GFP, AD-NAC1L or AD-NAC25 constructs. Diploid cells were grown on diploid (-L-W) and screening (-L-W-H) plates with or without 3-AT. **(D)** Coimmunoprecipitation (CoIP) assays with co-expressed HA-NAC25 and RGL2-GFP in leaves of *N. benthamiana*. Soluble protein extracts before (input) and after (IP α-HA) immunoprecipitation with an anti-HA antibody were subjected to inmunoblot with an anti-GFP^{HRP} antibody or an anti- HA^{HRP} antibody. **(E)** Diagram of the *EXPA2* promoter (reporter) and TF constructs (effectors) used for transient expression analyses in *N. benthamiana* leaves. *N. benthamiana* leaves were agroinfiltrated with the *ProEXPA2* construct together with each effector construct overexpressing NAC25 or/and RGL2. **(F)** Luciferase activity in *N. benthamiana* leaves agroinfiltrated with the *ProEXPA2:LUC* construct and effector constructs overexpressing the indicated TFs. When TFs were not combined and in the control lane, appropriate amounts of the empty effector plasmid (pCX) were co-infiltrated to equalize bacterial numbers between leaves. Averages and SE of luciferase activity from at least 4 replicates are shown and similar results were obtained in an additional agroinfiltration experiment. Asterisks represent significant differences at $P < 0.05$ (*) using the Mann-Whitney test (two-sided).

Figure 5. NAC TFs are positive regulators of germination, *CWRE* gene expression and mediate GA-responses. (A) Germination percentage of WT (Col-0) and NAC knock-out seeds at 48 hai. **(B)** Up and downregulated genes in the *nac25-1* and *nac1L-1* mutants represented in Venn diagrams. **(C)** Germination percentage of WT (Col-0) and NAC single (*nac25-1* and *nac1L-1*)

and double knock-out seeds at 48 hai. **(D)** Yeast strains containing the NAC25 or NAC1L CDS fused to the GAL4-BD (BD-NAC; bait) were mated to strains containing the AD-Ø, AD-GFP, AD-NAC1L or AD-NAC25 constructs. Diploid cells were grown on diploid (-L-W) and screening (-L-W-H) plates with or without 3-AT. **(E)** Overlap between genes downregulated >4-fold in the *nac25-1* transcriptome and genes deregulated >4-fold in GA-related transcriptomes. **(F)** NACbs sequence content in 500-bp promoters of genes downregulated >4-fold in the *nac25-1* mutant and those commonly deregulated in GA-related transcriptomes or belonging to the CWRE class. The average NACbs occurrence in the Arabidopsis gene promoters, Araport11 Loci Upstream Seq–500 bp, is taken arbitrarily as 1 (TAIR). Asterisks represent significant differences, at $P < 0.01$ (**) or $P < 0.05$ (*), from the control (TAIR) using the X^2-test. The results shown in **(A)** and **(C)** represent average values and SE for four biological replicates.

Figure 6. NAC25 and NAC1L TFs are positive regulators of testa rupture and endosperm cell expansion. (A) Percentage of testa rupture in WT and NAC loss-of-function mutant seeds at 27 and 32 hai. Average percentage and SE for at least 5 biological replicates are shown. **(B)** Cell surfaces per region of every genotype at 27 hai were compared to those calculated in samples at 6 hai in order to study cell elongation. Asterisks represent significant differences at $P < 0.01$ (**) and at $P < 0.05$ (*) using the Mann-Whitney test (two-sided).

Figure 7. Regulatory model for GA-mediated endosperm cell expansion. Our results suggest a regulatory model where RGL2 blocks GA-signaling in the endosperm by sequestering NACs. Upon imbibition, a signal from embryo and/or GA biosynthesis destabilizes RGL2 and releases NACs to activate *CWRE* gene expression, having an impact on endosperm cell elongation to accommodate embryo growth and facilitate radicle protrusion (germination *sensu stricto*).

SUPPLEMENTAL INFORMATION

Supplemental Figure 1. Visualization of changes in endosperm cells during Arabidopsis seed germination. **(A)** Semi-thin TBO sections of Arabidopsis endosperm cells at 3 hai. **(B)** Semi-thin TBO sections of Arabidopsis

endosperm cells at testa rupture. **(C)** Confocal image with GFP targeted to vacuole membrane before testa rupture. **(D)** Same as **(C)** after testa rupture.

Supplemental Figure 2. *ProEXPA2:GUS* embryo separated from endosperm at 24 hai and stained overnight to detect GUS activity.

Supplemental Figure 3. Conserved 80 bp sequenced (*EXPA2-CS*) found after alignment of orthologous *EXPA2* gene promoters from several plant species belonging to the *Brassicaceae* family.

Supplemental Figure 4. Y1H screening results and control baits. **(A)** Y1H assay using the *EXPA2-CS* bait and NAC25 (2-E5), NAC1L (12-G1) and two randomly selected library clones (2-A3 and 12-A6) as preys. **(B)** Y1H assay using the *LIP1-CS* bait and NAC25 and NAC1L as preys.

Supplemental Figure 5. RT-qPCR on RNA isolated from Arabidopsis Col-0 dissected embryos and endosperms at the indicated timepoints. *TCP14* and *MYB101* are expressed throughout imbibition almost exclusively in embryo and endosperm (Dekkers et al., 2013), respectively, and were used to detect significant amounts of tissue-cross contamination in the samples.

Supplemental Figure 6. Characterization of NAC25 and NAC1L single loss-of-function mutants. **(A)** Schematic representation of NAC knock out mutants and oligonucleotides used to amplify full-lenght cDNAs. **(B)** To check that no full-length NAC mRNAs were produced in the homozygous plants, PCR with oligonucleotides spanning the corresponding TDNA insertions was carried out on cDNAs synthetized from RNAs isolated at 12 hai (the same RNAs used for RNA-seq).

Supplemental Figure 7. NAC25 and NAC1L form homo and heterodimers *in planta*. **(A)** The NAC25 and NAC1L CDSs were fused to the N-YFP (N) or C-CFP (C) CDS and coexpressed in *N. benthamiana* cells in different combinations as indicated in the table. Empty vectors (Ø) were included in the combinations as controls. Combinations giving a fluorescent signal in the nuclei of *N. benthamiana* cells or not giving any signal are indicated as (+) and (-), respectively. **(B)** Images obtained in a fluorescence microscope for several combinations showing nuclear fluorescence.

Supplemental Figure 8. Quantification of *CWRE* Gene Expression in NAC knock-out mutants. Quantification by qRT-PCR of mRNA levels of *CWREs* and control genes (ICL and MLS) in wild-type, *nac25-1*, *nac25-2*, *nac1L-1* and

nac1L-2 genotypes. RNAs were isolated from seeds at 12 hai, and their levels are shown relative to those of *ACT8*. Average values and SE for two replicates are shown. Similar results were obtained with a different seed batch.

Supplemental Figure 9. Overlap between genes downregulated >2-fold in the *nac25-1* transcriptome and genes deregulated >2-fold in GA-related transcriptomes.

Supplemental Figure 10. Quantification of *EXPA2* gene expression in WT and *ProML1:GFP-gai-1* seeds, the latter ones having blocked GA signaling in the epidermis (Gallego-Bartolomé et al., 2011; Rombolá-Caldentey et al., 2014).

Supplemental Table 1. List of Oligonucleotides Used.

Supplemental Table 2. List of deregulated genes in *nac25-1* and *nac1L-1* mutants compared to Col-0 at 12 hai.

Supplemental Table 3. GO enrichment for biological processes according to GeneCodis (529 genes downregulated >4-fold in *nac25-1*). Gene groups with a p value < 10^{-6} were classified according to their fold enrichments.

Supplemental Table 4. Cell wall remodelling genes significantly downregulated over 2-fold in the *nac25-1* mutant.

Supplemental Table 5. Transcription factors downregulated over 4 fold in the *nac25-1* mutant.

Supplemental Table 6. Sample information from the sequence quality control report.

REFERENCES

Afgan, E., Baker, D., van den Beek, M., Blankenberg, D., Bouvier, D., Cech, M., Chilton, J., Clements, D., Coraor, N., Eberhard, C., Gruning, B., Guerler, A., Hillman-Jackson, J., Von Kuster, G., Rasche, E., Soranzo, N., Turaga, N., Taylor, J., Nekrutenko, A., and Goecks, J. (2016). The Galaxy platform for accessible, reproducible and collaborative biomedical analyses: 2016 update. Nucleic Acids Res. **44**:W3-W10.

Barbier de Reuille, P., Routier-Kierzkowska, A.-L., Kierzkowski, D., Bassel, G.W., Schüpbach, T., Tauriello, G., Bajpai, N., Strauss, S., Weber, A., Kiss, A., Burian, A., Hofhuis, H., Sapala, A., Lipowczan, M., Heimlicher, M.B., Robinson, S., Bayer, E.M., Basler, K., Koumoutsakos, P., Roeder, A.H.K.,

Aegerter-Wilmsen, T., Nakayama, N., Tsiantis, M., Hay, A., Kwiatkowska, D., Xenarios, I., Kuhlemeier, C., and Smith, R.S. (2015). MorphoGraphX: A platform for quantifying morphogenesis in 4D. eLife **4**:e05864.

Bassel, G.W. (2016). To Grow or not to Grow? Trends Plant Sci. **21**:498-505.

Bassel, G.W., Mullen, R.T., and Bewley, J.D. (2006). ABI3 expression ceases following, but not during, germination of tomato and Arabidopsis seeds. J. Exp. Bot. **57**:1291-1297.

Bassel, G.W., Stamm, P., Mosca, G., Barbier de Reuille, P., Gibbs, D.J., Winter, R., Janka, A., Holdsworth, M.J., and Smith, R.S. (2014). Mechanical constraints imposed by 3D cellular geometry and arrangement modulate growth patterns in the Arabidopsis embryo. Proc. Natl. Acad. Sci. USA **111**:8685-8690.

Bethke, P.C., Libourel, I.G., Aoyama, N., Chung, Y.Y., Still, D.W., and Jones, R.L. (2007). The Arabidopsis aleurone layer responds to nitric oxide, gibberellin, and abscisic acid and is sufficient and necessary for seed dormancy. Plant Physiol. **143**:1173-1188.

Cao, D., Hussain, A., Cheng, H., and Peng, J. (2005). Loss of function of four DELLA genes leads to light- and gibberellin-independent seed germination in Arabidopsis. Planta **223**:105-113.

Cao, D., Cheng, H., Wu, W., Soo, H.M., and Peng, J. (2006). Gibberellin mobilizes distinct DELLA-dependent transcriptomes to regulate seed germination and floral development in Arabidopsis. Plant Physiol. **142**:509-525.

Castrillo, G., Turck, F., Leveugle, M., Lecharny, A., Carbonero, P., Coupland, G., Paz-Ares, J., and Oñate-Sánchez, L. (2011). Speeding cis-trans regulation discovery by phylogenomic analyses coupled with screenings of an arrayed library of Arabidopsis transcription factors. PLoS One **6**:e21524.

Chen, F., and Bradford, K.J. (2000). Expression of an expansin is associated with endosperm weakening during tomato seed germination. Plant Physiol. **124**:1265-1274.

Chen, F., Nonogaki, H., and Bradford, K.J. (2002). A gibberellin-regulated xyloglucan endotransglycosylase gene is expressed in the endosperm cap during tomato seed germination. J. Exp. Bot. **53**:215-223.

Chen, W., and Singh, K.B. (1999). The auxin, hydrogen peroxide and salicylic acid induced expression of the Arabidopsis GST6 promoter is mediated in part by an ocs element. Plant J. **19**:667-677.

Clough, S.J., and Bent, A.F. (1998). Floral dip: a simplified method for Agrobacterium-mediated transformation of Arabidopsis thaliana. Plant J. **16**:735-743.

Coen, E., Rolland-Lagan, A.-G., Matthews, M., Bangham, J.A., and Prusinkiewicz, P. (2004). The genetics of geometry. Proc. Natl. Acad. Sci. USA **101**:4728.

Cosgrove, D.J. (2015). Plant expansins: diversity and interactions with plant cell walls. Curr. Opin. Plant Biol. **25**:162-172.

Cutler, S.R., Ehrhardt, D.W., Griffitts, J.S., and Somerville, C.R. (2000). Random GFP::cDNA fusions enable visualization of subcellular structures in cells of Arabidopsis at a high frequency. Proc. Natl. Acad. Sci. USA **97**:3718.

De Giorgi, J., Piskurewicz, U., Loubery, S., Utz-Pugin, A., Bailly, C., Mene-Saffrane, L., and Lopez-Molina, L. (2015). An endosperm-associated cuticle is required for Arabidopsis seed viability, dormancy and early control of germination. PLoS Genet. **11**:e1005708.

Dekkers, B.J., Pearce, S., van Bolderen-Veldkamp, R.P., Marshall, A., Widera, P., Gilbert, J., Drost, H.G., Bassel, G.W., Muller, K., King, J.R., Wood, A.T., Grosse, I., Quint, M., Krasnogor, N., Leubner-Metzger, G., Holdsworth, M.J., and Bentsink, L. (2013). Transcriptional dynamics of two seed compartments with opposing roles in Arabidopsis seed germination. Plant Physiol. **163**:205-215.

Duan, L., Dietrich, D., Ng, C.H., Chan, P.M., Bhalerao, R., Bennett, M.J., and Dinneny, J.R. (2013). Endodermal ABA signaling promotes lateral root quiescence during salt stress in Arabidopsis seedlings. Plant Cell **25**:324-341.

Dubreucq, B., Berger, N., Vincent, E., Boisson, M., Pelletier, G., Caboche, M., and Lepiniec, L. (2000). The Arabidopsis AtEPR1 extensin-like gene is specifically expressed in endosperm during seed germination. Plant J. **23**:643-652.

Edwards, K., Johnstone, C., and Thompson, C. (1991). A simple and rapid method for the preparation of plant genomic DNA for PCR analysis. Nucleic Acids Res. **19**:1349.

Endo, A., Tatematsu, K., Hanada, K., Duermeyer, L., Okamoto, M., Yonekura-Sakakibara, K., Saito, K., Toyoda, T., Kawakami, N., Kamiya, Y.,

Seki, M., and Nambara, E. (2012). Tissue-specific transcriptome analysis reveals cell wall metabolism, flavonol biosynthesis and defense responses are activated in the endosperm of germinating Arabidopsis thaliana seeds. Plant Cell Physiol. **53**:16-27.

Espinosa-Ruiz, A., Martínez, C., de Lucas, M., Fábregas, N., Bosch, N., Caño-Delgado, A.I., and Prat, S. (2017). TOPLESS mediates brassinosteroid control of shoot boundaries and root meristem development in Arabidopsis thaliana. Development **144**:1619-1628.

Finch-Savage, W.E., and Leubner-Metzger, G. (2006). Seed dormancy and the control of germination. New Phytol. **171:**501-523.

Finch-Savage, W.E., and Bassel, G.W. (2016). Seed vigour and crop establishment: extending performance beyond adaptation. J. Exp. Bot. **67**:567-591.

Franco-Zorrilla, J.M., Lopez-Vidriero, I., Carrasco, J.L., Godoy, M., Vera, P., and Solano, R. (2014). DNA-binding specificities of plant transcription factors and their potential to define target genes. Proc. Natl. Acad. Sci. USA **111**:2367-2372.

Geng, Y., Wu, R., Wee, C.W., Xie, F., Wei, X., Chan, P.M., Tham, C., Duan, L., and Dinneny, J.R. (2013). A spatio-temporal understanding of growth regulation during the salt stress response in Arabidopsis. Plant Cell **25**:2132-2154.

Groot, S.P., and Karssen, C.M. (1987). Gibberellins regulate seed germination in tomato by endosperm weakening: a study with gibberellin-deficient mutants. Planta **171**:525-531.

Groot, S.P.C., Kieliszewska-Rokicka, B., Vermeer, E., and Karssen, C.M. (1988). Gibberellin-induced hydrolysis of endosperm cell walls in gibberellin-deficient tomato seeds prior to radicle protrusion. Planta **174**:500-504.

Gubler, F., and Jacobsen, J.V. (1992). Gibberellin-responsive elements in the promoter of a barley high-pI alpha-amylase gene. Plant Cell **4**:1435-1441.

Heo, J.O., Chang, K.S., Kim, I.A., Lee, M.H., Lee, S.A., Song, S.K., Lee, M.M., and Lim, J. (2011). Funneling of gibberellin signaling by the GRAS transcription regulator scarecrow-like 3 in the Arabidopsis root. Proc. Natl. Acad. Sci. USA **108**:2166-2171.

Holdsworth, M.J., Bentsink, L., and Soppe, W.J. (2008). Molecular networks regulating Arabidopsis seed maturation, after-ripening, dormancy and germination. New Phytol. **179**:33-54.

Karimi M, Inzé D, Depicker A (2002). GATEWAY vectors for Agrobacterium-mediated plant transformation. Trends Plant Sci. **7**:193-195.

Koornneef, M., and van der Veen, J.H. (1980). Induction and analysis of gibberellin sensitive mutants in Arabidopsis thaliana (L.) heynh. Theor. Appl. Genet. **58**:257-263.

Langmead, B., Trapnell, C., Pop, M., and Salzberg, S.L. (2009). Ultrafast and memory-efficient alignment of short DNA sequences to the human genome. Genome Biol. **10**:R25.

Lee, K.J., Dekkers, B.J., Steinbrecher, T., Walsh, C.T., Bacic, A., Bentsink, L., Leubner-Metzger, G., and Knox, J.P. (2012a). Distinct cell wall architectures in seed endosperms in representatives of the Brassicaceae and Solanaceae. Plant Physiol. **160**:1551-1566.

Lee, K.P., Piskurewicz, U., Tureckova, V., Strnad, M., and Lopez-Molina, L. (2010). A seed coat bedding assay shows that RGL2-dependent release of abscisic acid by the endosperm controls embryo growth in Arabidopsis dormant seeds. Proc. Natl. Acad. Sci. USA **107**:19108-19113.

Lee, K.P., Piskurewicz, U., Tureckova, V., Carat, S., Chappuis, R., Strnad, M., Fankhauser, C., and Lopez-Molina, L. (2012b). Spatially and genetically distinct control of seed germination by phytochromes A and B. Genes Dev. **26**:1984-1996.

Lee, S., Cheng, H., King, K.E., Wang, W., He, Y., Hussain, A., Lo, J., Harberd, N.P., and Peng, J. (2002). Gibberellin regulates Arabidopsis seed germination via RGL2, a GAI/RGA-like gene whose expression is up-regulated following imbibition. Genes Dev. **16**:646-658.

Lofke, C., Zwiewka, M., Heilmann, I., Van Montagu, M.C., Teichmann, T., and Friml, J. (2013). Asymmetric gibberellin signaling regulates vacuolar trafficking of PIN auxin transporters during root gravitropism. Proc. Natl. Acad. Sci. USA **110**:3627-3632.

Martínez-Andújar, C., Pluskota, W.E., Bassel, G.W., Asahina, M., Pupel, P., Nguyen, T.T., Takeda-Kamiya, N., Toubiana, D., Bai, B., Gorecki, R.J., Fait, A., Yamaguchi, S., and Nonogaki, H. (2012). Mechanisms of hormonal

regulation of endosperm cap-specific gene expression in tomato seeds. Plant J. **71**:575-586.

Morris, K., Linkies, A., Muller, K., Oracz, K., Wang, X., Lynn, J.R., Leubner-Metzger, G., and Finch-Savage, W.E. (2011). Regulation of seed germination in the close Arabidopsis relative Lepidium sativum: a global tissue-specific transcript analysis. Plant Physiol. **155**:1851-1870.

Müller, K., Tintelnot, S., and Leubner-Metzger, G. (2006). Endosperm-limited Brassicaceae seed germination: abscisic acid inhibits embryo-induced endosperm weakening of Lepidium sativum (cress) and endosperm rupture of Cress and Arabidopsis thaliana. Plant Cell Physiol. **47**:864-877.

Ogawa, M., Hanada, A., Yamauchi, Y., Kuwahara, A., Kamiya, Y., and Yamaguchi, S. (2003). Gibberellin biosynthesis and response during Arabidopsis seed germination. Plant Cell **15**:1591-1604.

Oñate-Sánchez, L., and Vicente-Carbajosa, J. (2008). DNA-free RNA isolation protocols for Arabidopsis thaliana, including seeds and siliques. BMC Res. Notes **1**:93.

Penfield, S., Li, Y., Gilday, A.D., Graham, S., and Graham, I.A. (2006). Arabidopsis ABA INSENSITIVE4 regulates lipid mobilization in the embryo and reveals repression of seed germination by the endosperm. Plant Cell **18**:1887-1899.

Penfield, S., Rylott, E.L., Gilday, A.D., Graham, S., Larson, T.R., and Graham, I.A. (2004). Reserve mobilization in the Arabidopsis endosperm fuels hypocotyl elongation in the dark, is independent of abscisic acid, and requires PHOSPHOENOLPYRUVATE CARBOXYKINASE1. Plant Cell **16**:2705-2718.

Puranik, S., Sahu, P.P., Srivastava, P.S., and Prasad, M. (2012). NAC proteins: regulation and role in stress tolerance. Trends Plant Sci. **17**:369-381.

Rombolá-Caldentey, B., Rueda-Romero, P., Iglesias-Fernández, R., Carbonero, P., and Oñate-Sánchez, L. (2014). Arabidopsis DELLA and two HD-ZIP transcription factors regulate GA signaling in the epidermis through the L1 box cis-element. Plant Cell **26**:2905-2919.

Sánchez-Montesino, R. and Oñate-Sánchez, L. (2017). Yeast one- and two-hybrid high-throughput screenings using arrayed libraries. In K. Kaufmann and B. Mueller-Roeber (eds.), Plant Gene Regulatory Networks (Humana Press, New York, NY). Methods Mol. Biol. **1629**:47-65.

Sánchez-Montesino, R., and Oñate-Sánchez, L. (2018). Screening arrayed libraries with DNA and protein baits to identify interacting proteins. In L. Oñate-Sánchez, (ed.), Two-Hybrid Systems (Humana Press, New York, NY). Methods Mol. Biol. **1794**:131-149.

Scheler, C., Weitbrecht, K., Pearce, S., Hampstead, A., Büttner-Mainik, A., Lee, K. J. D., Voegele, A., Oracz, K., Dekkers, B. J. W., Wang, X., Wood, A., Bentsink, L., King, J. R., Knox, P., Holdsworth, M., Müller, K. and Leubner-Metzger, G (2015) Promotion of testa rupture during Lepidium sativum germination involves seed compartment-specific expression and activity of pectin methylesterases. Plant Physiol. **167**:200-215.

Sechet, J., Frey, A., Effroy-Cuzzi, D., Berger, A., Perreau, F., Cueff, G., Charif, D., Rajjou, L., Mouille, G., North, H.M., and Marion-Poll, A. (2016). Xyloglucan Metabolism Differentially Impacts the Cell Wall Characteristics of the Endosperm and Embryo during Arabidopsis Seed Germination. Plant Physiol. **170**:1367-1380.

Skriver, K., Olsen, F.L., Rogers, J.C., and Mundy, J. (1991). cis-acting DNA elements responsive to gibberellin and its antagonist abscisic acid. Proc. Natl. Acad. Sci. USA **88**:7266-7270.

Sliwinska, E., Bassel, G.W., and Bewley, J.D. (2009). Germination of Arabidopsis thaliana seeds is not completed as a result of elongation of the radicle but of the adjacent transition zone and lower hypocotyl. J. Exp. Bot. **60**:3587-3594.

Stamm, P., Ravindran, P., Mohanty, B., Tan, E.L., Yu, H., and Kumar, P.P. (2012). Insights into the molecular mechanism of RGL2-mediated inhibition of seed germination in Arabidopsis thaliana. BMC Plant Biol. **12**:179.

Stamm, P., Topham, A.T., Mukhtar, N.K., Jackson, M.D., Tome, D.F., Beynon, J.L., and Bassel, G.W. (2017). The Transcription Factor ATHB5 Affects GA-Mediated Plasticity in Hypocotyl Cell Growth during Seed Germination. Plant Physiol. **173**:907-917.

Steinbrecher, T., and Leubner-Metzger, G. (2016). The biomechanics of seed germination. J. Exp. Bot. **68**:765-783.

Sun, T.P., and Kamiya, Y. (1994). The Arabidopsis GA1 locus encodes the cyclase ent-kaurene synthetase A of gibberellin biosynthesis. Plant Cell **6**:1509-1518.

Trapnell, C., Williams, B.A., Pertea, G., Mortazavi, A., Kwan, G., van Baren, M.J., Salzberg, S.L., Wold, B.J., and Pachter, L. (2010). Transcript assembly and quantification by RNA-Seq reveals unannotated transcripts and isoform switching during cell differentiation. Nat. Biotechnol. **28**:511.

Tyler, L., Thomas, S.G., Hu, J., Dill, A., Alonso, J.M., Ecker, J.R., and Sun, T.P. (2004). Della proteins and gibberellin-regulated seed germination and floral development in Arabidopsis. Plant Physiol. **135**:1008-1019.

Ubeda-Tomas, S., Swarup, R., Coates, J., Swarup, K., Laplaze, L., Beemster, G.T., Hedden, P., Bhalerao, R., and Bennett, M.J. (2008). Root growth in Arabidopsis requires gibberellin/DELLA signalling in the endodermis. Nat. Cell Biol. **10**:625-628.

Voinnet, O., Rivas, S., Mestre, P., and Baulcombe, D. (2003). An enhanced transient expression system in plants based on suppression of gene silencing by the p19 protein of tomato bushy stunt virus. Plant J. **33**:949-956.

Yamada, K., Lim, J., Dale, J.M., Chen, H., Shinn, P., Palm, C.J., Southwick, A.M., Wu, H.C., Kim, C., Nguyen, M., Pham, P., Cheuk, R., Karlin-Newmann, G., Liu, S.X., Lam, B., Sakano, H., Wu, T., Yu, G., Miranda, M., Quach, H.L., Tripp, M., Chang, C.H., Lee, J.M., Toriumi, M., Chan, M.M., Tang, C.C., Onodera, C.S., Deng, J.M., Akiyama, K., Ansari, Y., Arakawa, T., Banh, J., Banno, F., Bowser, L., Brooks, S., Carninci, P., Chao, Q., Choy, N., Enju, A., Goldsmith, A.D., Gurjal, M., Hansen, N.F., Hayashizaki, Y., Johnson-Hopson, C., Hsuan, V.W., Iida, K., Karnes, M., Khan, S., Koesema, E., Ishida, J., Jiang, P.X., Jones, T., Kawai, J., Kamiya, A., Meyers, C., Nakajima, M., Narusaka, M., Seki, M., Sakurai, T., Satou, M., Tamse, R., Vaysberg, M., Wallender, E.K., Wong, C., Yamamura, Y., Yuan, S., Shinozaki, K., Davis, R.W., Theologis, A., and Ecker, J.R. (2003). Empirical analysis of transcriptional activity in the Arabidopsis genome. Science **302**:842-846.

Yan, A., Wu, M., Yan, L., Hu, R., Ali, I., and Gan, Y. (2014a). AtEXP2 is involved in seed germination and abiotic stress response in Arabidopsis. PLoS One **9**:e85208.

Yan, D., Duermeyer, L., Leoveanu, C., and Nambara, E. (2014b). The functions of the endosperm during seed germination. Plant Cell Physiol. **55**:1521-1533.

Zhang, Z.L., Ogawa, M., Fleet, C.M., Zentella, R., Hu, J., Heo, J.O., Lim, J., Kamiya, Y., Yamaguchi, S., and Sun, T.P. (2011). Scarecrow-like 3 promotes gibberellin signaling by antagonizing master growth repressor DELLA in Arabidopsis. Proc. Natl. Acad. Sci. USA **108**:2160-2165.

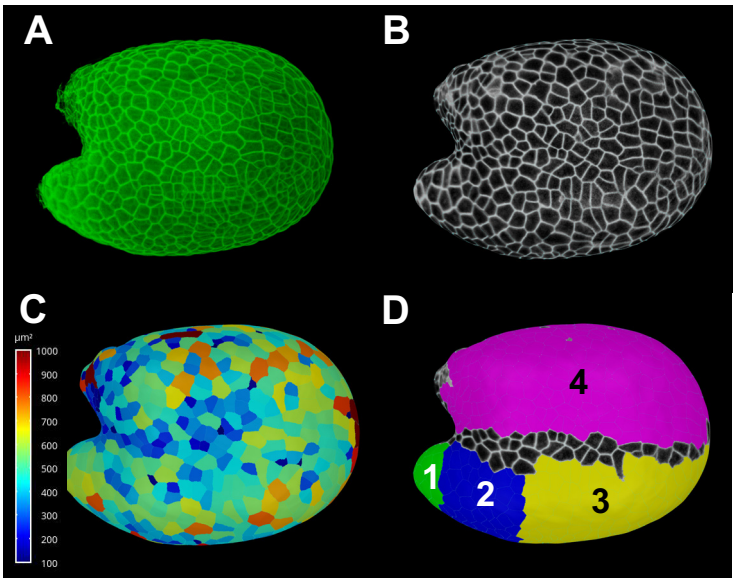
A
B
C
D
μm²
1000
900
800
700
600
500
400
300
200
100
1
2
3
4

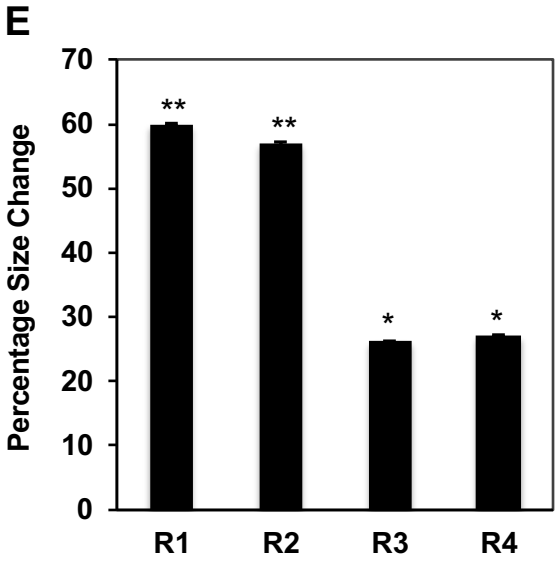
E
Percentage Size Change
70
60
50
40
30
20
10
0
**
**
*
*
R1
R2
R3
R4

Figure 1

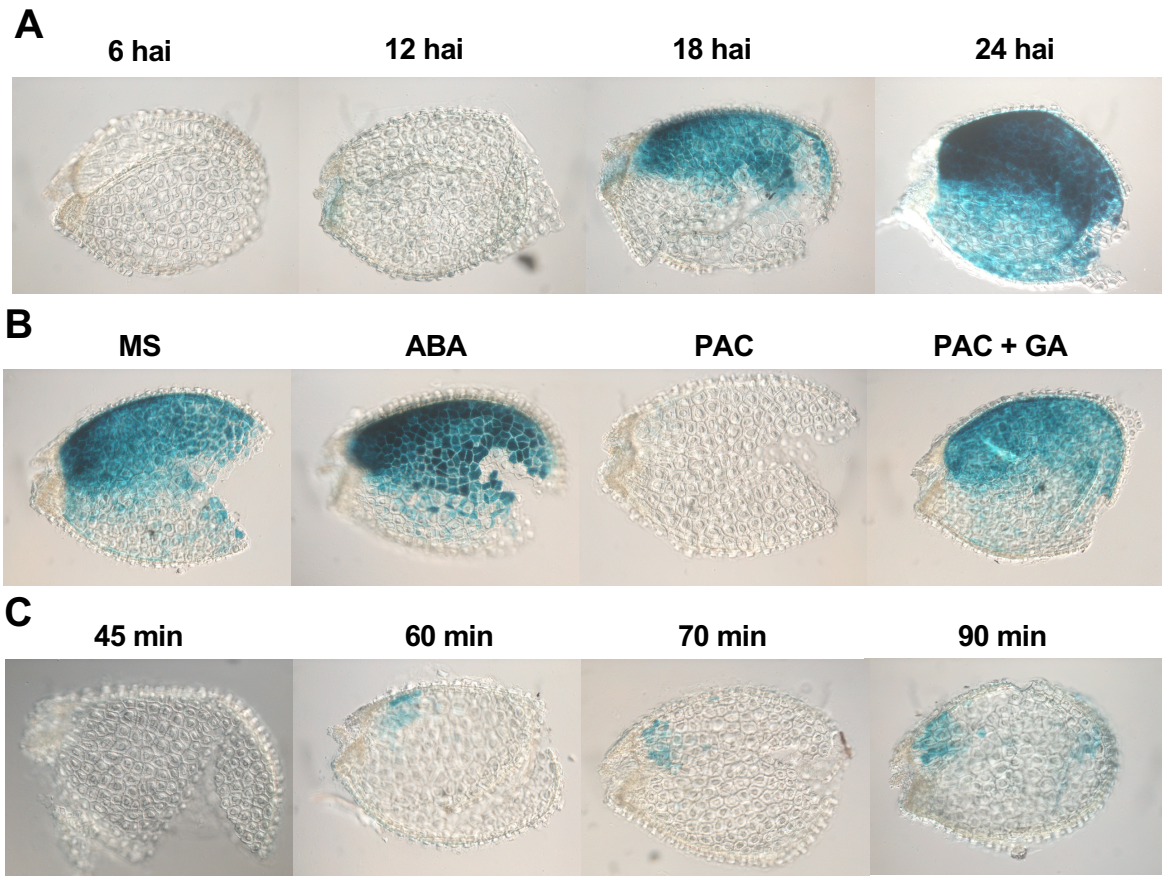
A
6 hai
12 hai
18 hai
24 hai
B
MS
ABA
PAC
PAC + GA
C
45 min
60 min
70 min
90 min

Figure 2

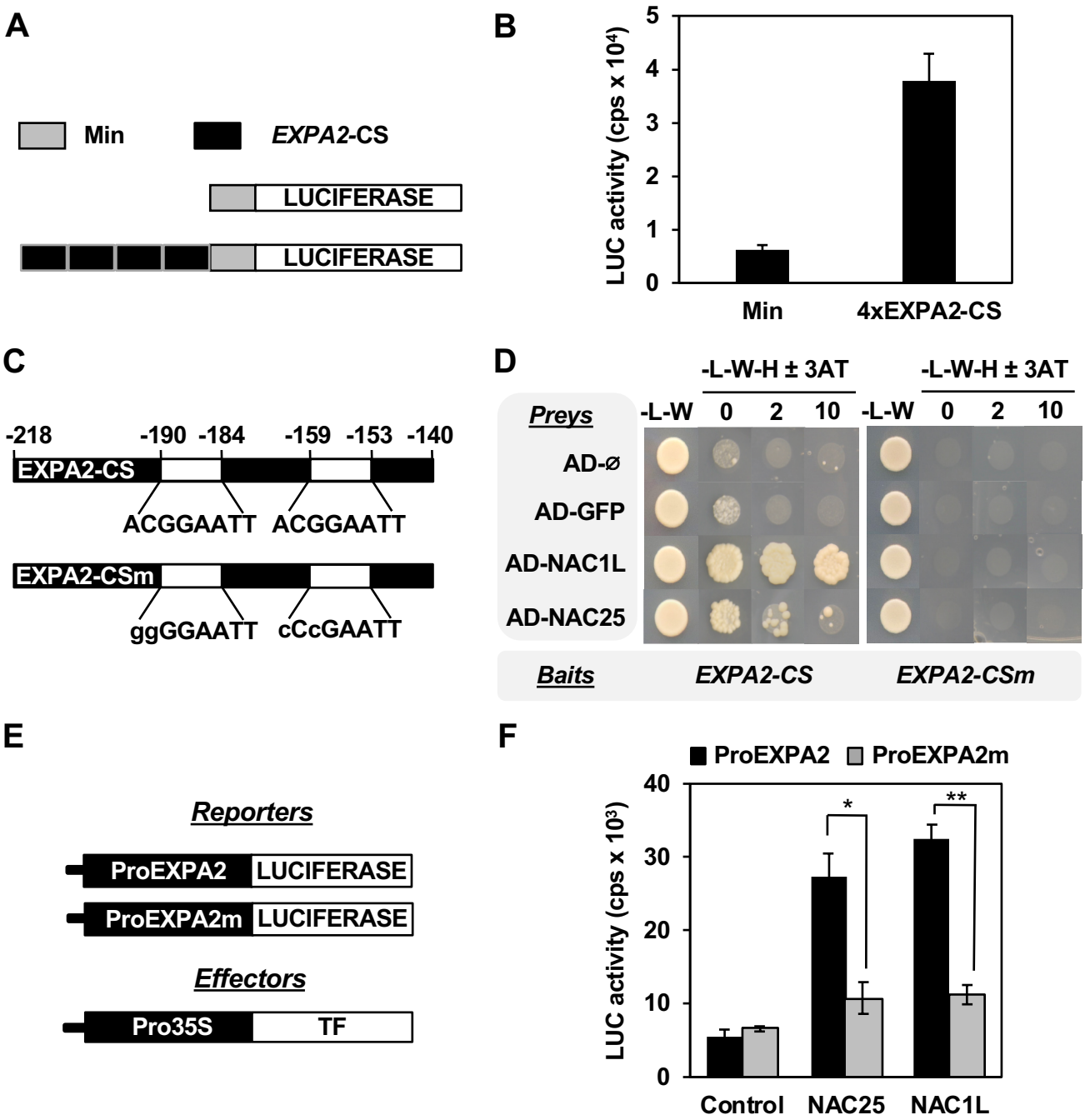
A
Min
EXPA2-CS
LUCIFERASE
LUCIFERASE
B
LUC activity (cps x 10⁴)
5
4
3
2
1
0
Min
4xEXPA2-CS
C
-218
-190
-184
-159
-153
-140
EXPA2-CS
ACGGAATT
ACGGAATT
EXPA2-CSm
ggGGAATT
cCcGAATT
D
-L-W-H ± 3AT
-L-W-H ± 3AT
Preys
-L-W
0
2
10
-L-W
0
2
10
AD-ø
AD-GFP
AD-NAC1L
AD-NAC25
Baits
EXPA2-CS
EXPA2-CSm
E
Reporters
ProEXPA2
LUCIFERASE
ProEXPA2m
LUCIFERASE
Effectors
Pro35S
TF
F
ProEXPA2
ProEXPA2m
LUC activity (cps x 10³)
40
30
20
10
0
*
**
Control
NAC25
NAC1L

Figure 3

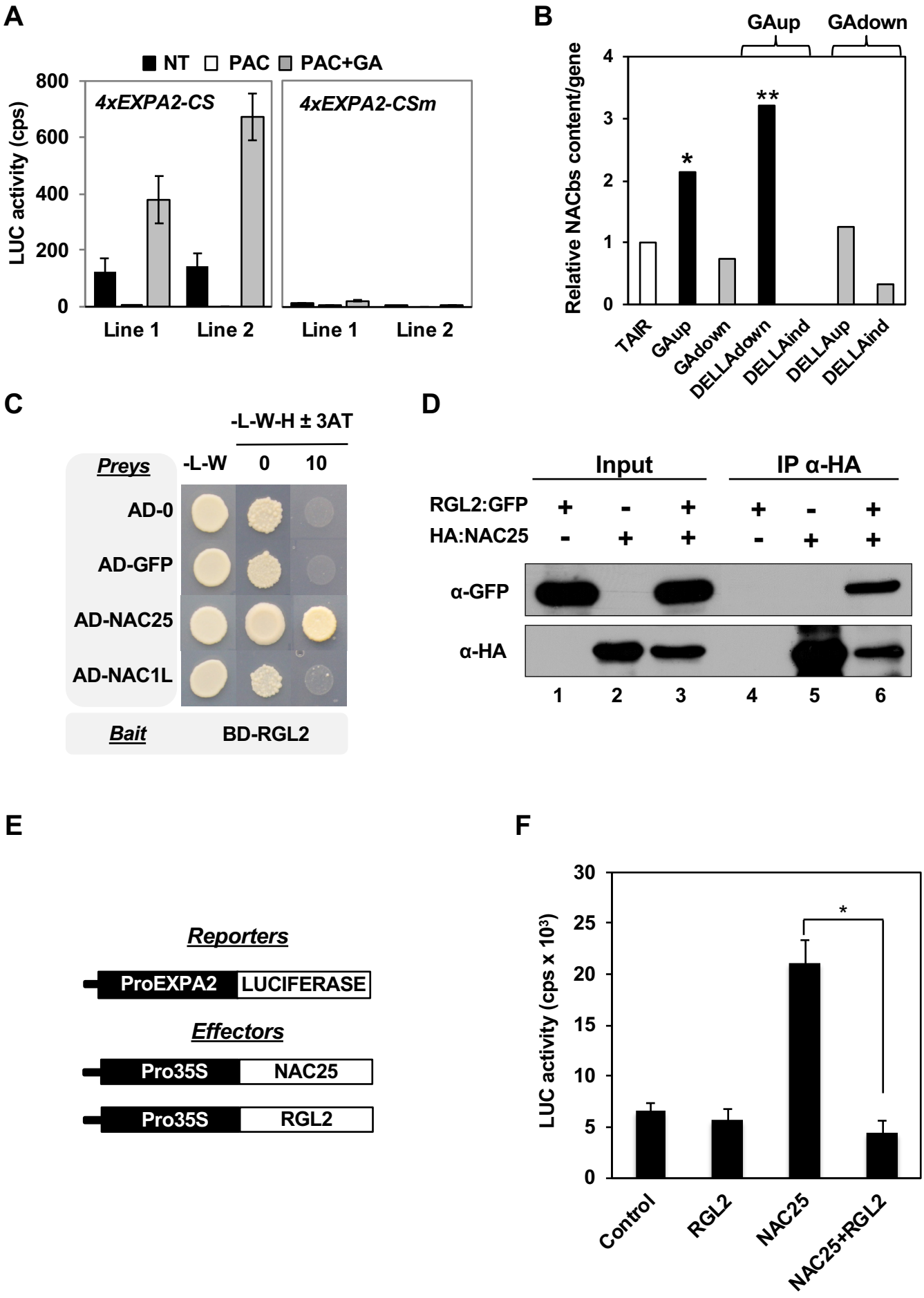
A
NT
PAC
PAC+GA
LUC activity (cps)
800
600
400
200
0
4xEXPA2-CS
4xEXPA2-CSm
Line 1
Line 2
Line 1
Line 2
B
GAup
GAdown
Relative NACbs content/gene
4
3
2
1
0
*
**
TAIR
GAup
GAdown
DELLAdown
DELLAind
DELLAup
DELLAind
C
-L-W-H ± 3AT
Preys
-L-W
0
10
AD-0
AD-GFP
AD-NAC25
AD-NAC1L
Bait
BD-RGL2
D
Input
IP α-HA
RGL2:GFP
HA:NAC25
α-GFP
α-HA
1
2
3
4
5
6
E
Reporters
ProEXPA2
LUCIFERASE
Effectors
Pro35S
NAC25
Pro35S
RGL2
F
LUC activity (cps x 10³)
30
25
20
15
10
5
0
*
Control
RGL2
NAC25
NAC25+RGL2

Figure 4

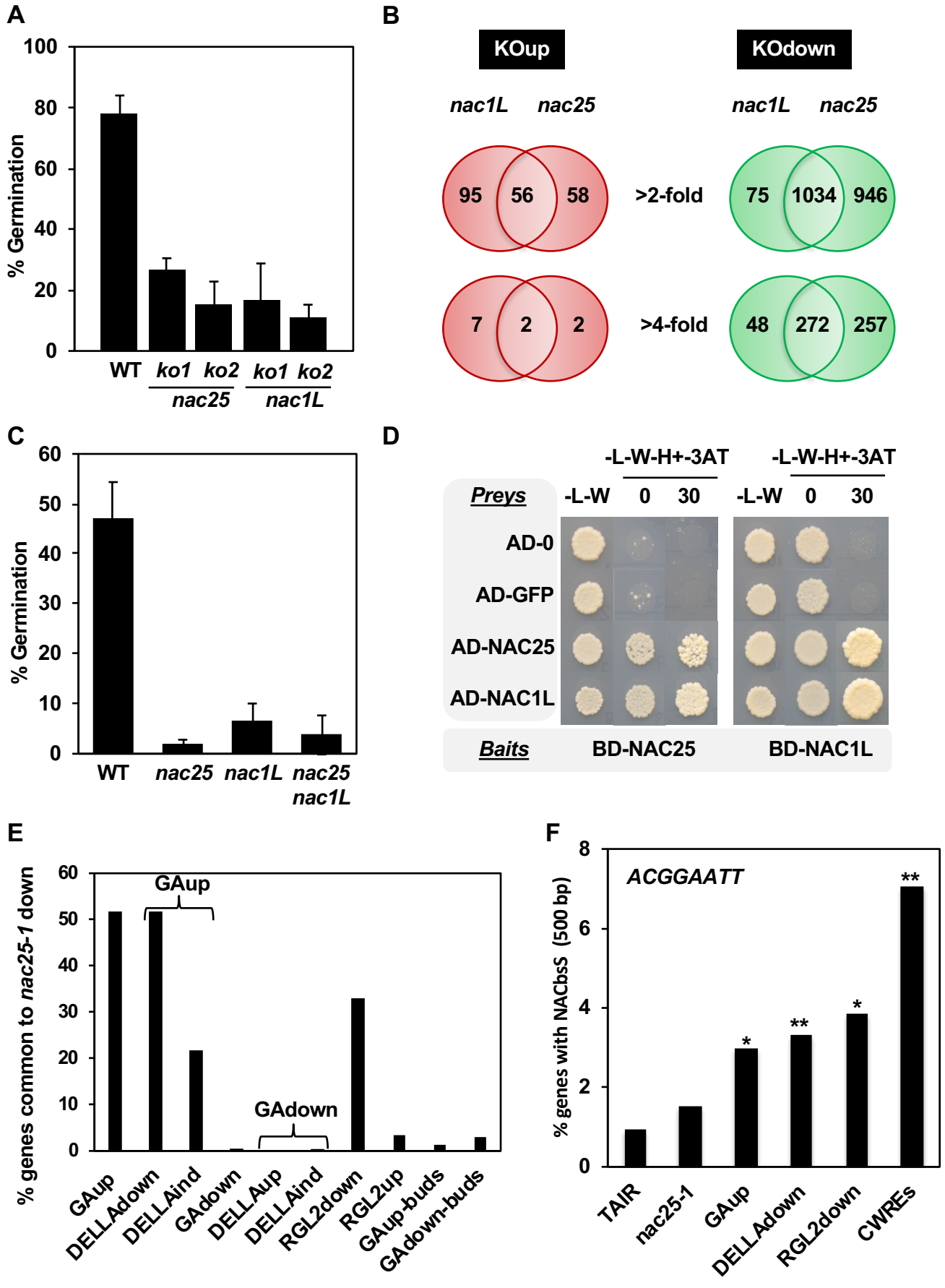
A
% Germination
WT
ko1
ko2
nac25
ko1
ko2
nac1L
B
KOup
KOdown
nac1L
nac25
95
56
58
>2-fold
75
1034
946
7
2
2
>4-fold
48
272
257
C
% Germination
WT
nac25
nac1L
nac25 nac1L
D
-L-W-H+-3AT
-L-W
0
30
Preys
AD-0
AD-GFP
AD-NAC25
AD-NAC1L
Baits
BD-NAC25
BD-NAC1L
E
% genes common to nac25-1 down
GAup
GAdown
GAup
DELLAdown
DELLAind
GAdown
DELLAup
DELLAind
RGL2down
RGL2up
GAup-buds
GAdown-buds
F
% genes with NACbsS (500 bp)
ACGGAATT
TAIR
nac25-1
GAup
DELLAdown
RGL2down
CWREs

Figure 5

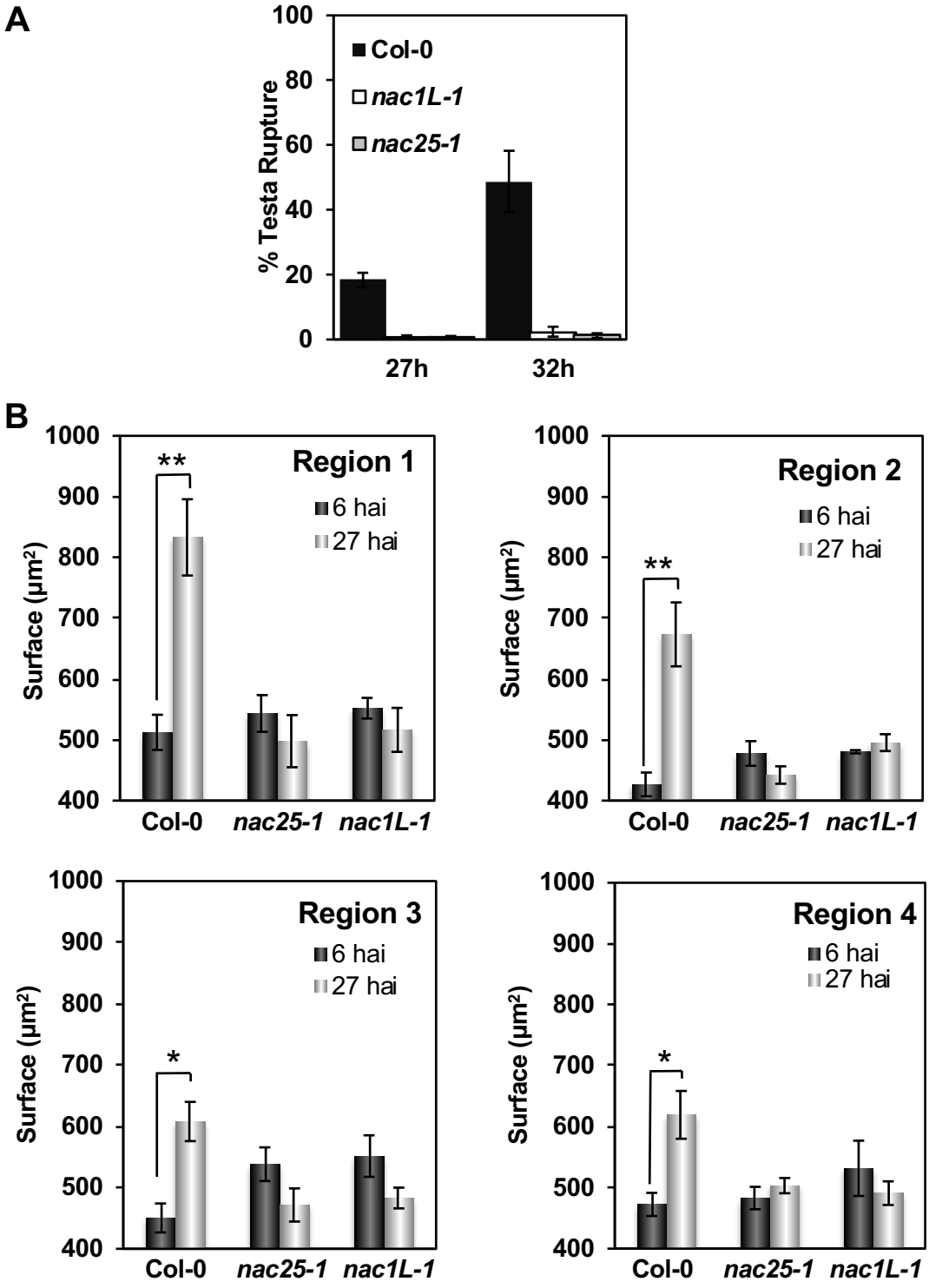
A
% Testa Rupture
Col-0
nac1L-1
nac25-1
27h
32h
B
Region 1
Region 2
Region 3
Region 4
6 hai
27 hai
Surface (µm²)
Col-0
nac25-1
nac1L-1
**
*

Figure 6

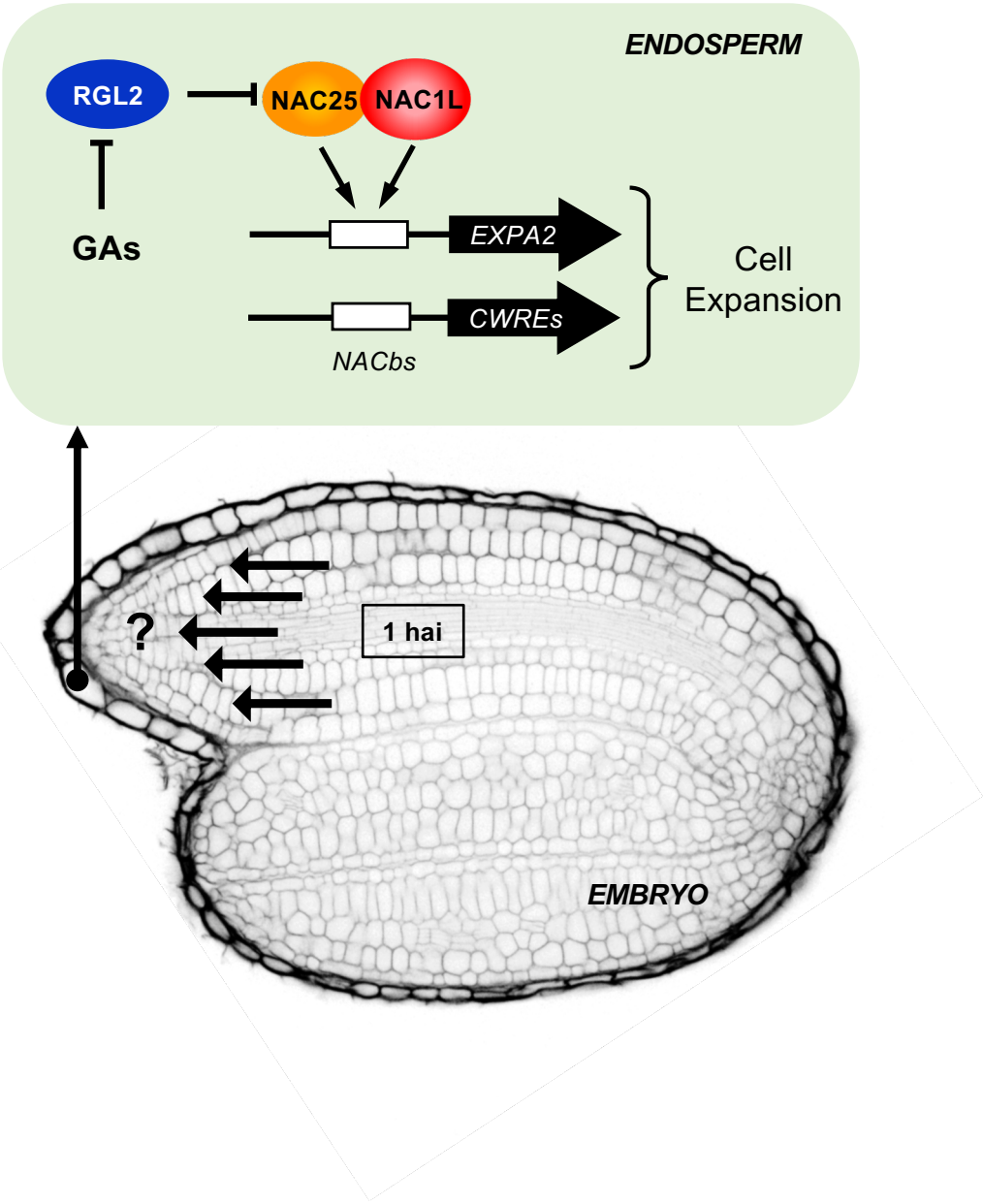
ENDOSPERM
RGL2
NAC25
NAC1L
GAs
EXPA2
CWREs
NACbs
Cell
Expansion
?
1 hai
EMBRYO

Figure 7